NJC

PAPER

Cite this: *New J. Chem.*, 2019, **43**, 3673

Self-assembly of cucurbiturils and cyclodextrins to supramolecular millstones with naphthalene derivatives capable of translocations in the host cavities†

Artem I. Vedernikov,[a] Natalia A. Lobova,[a] Lyudmila G. Kuz'mina,[b] Marina V. Fomina,[a] Yuri A. Strelenko,[c] Judith A. K. Howard[d] and Sergey P. Gromov *[ae]

Received 14th September 2018,
Accepted 22nd January 2019

DOI: 10.1039/c8nj04685a

rsc.li/njc

Quaternary 4-(2-naphthyl)pyridinium salts with various *N*-substituents were synthesized. The structure of these salts was determined by X-ray crystallography. The self-assembly of the salts with cavitand molecules – β- and γ-cyclodextrins and cucurbit[7,8]urils – in aqueous solutions was studied by electronic spectroscopy and ^{1}H NMR spectroscopy, including spectrophotometric, fluorescence, and ^{1}H NMR titrations. The formation of inclusion complexes of different stoichiometry and stability, was observed, depending on the structure of *N*-substituent in the quaternary salt and the cavitand nature and cavity size. The complex formation with cucurbiturils results in considerable changes in the absorption and fluorescence spectra of naphthylpyridine derivatives. Motion of the guest molecules in the cavitand cavities was detected. The X-ray diffraction study was carried out for two polymorphs of 2 : 1 complexes formed by betaine type naphthylpyridine and cucurbit[8]uril, in which the cavitand was located either above the naphthalene residues of a dimeric pair of guest molecules or above the centers of their conjugated moieties.

Introduction

Connection of organic molecules through various types of weak (non-covalent) interactions to form intricately structured assemblies is the subject of research of modern supramolecular chemistry.[1] In these assemblies, physical processes and chemical reactions that are not inherent in individual components are often allowed.[2]

Of particular interest are self-assemblies involving cavitand molecules (hosts) such as cyclodextrins (CD) and cucurbit[*n*]urils (CB[*n*], *n* = 5–8), which have relatively rigid cavities suitable for inclusion of one or two rather small organic guest molecules.[3] The formation of inclusion complexes of chromo- or luminogenic compounds with cavitands often induces considerable changes in their spectral and physicochemical properties. For example, the formation of 4-(2-naphthyl)pyridine complexes with β-CD and its 2-hydroxypropyl derivative suppresses the photoinduced protonation of the guest.[4] The complex formation between organic fluorophores and CD or CB[*n*] often leads to considerable fluorescence enhancement[2c,5] and to increasing photostability of fluorophores,[5a,6] while the formation of 2 : 1 complexes between unsaturated compounds and CB[8] or γ-CD is favorable for the stereo- and regioselective [2+2]-photocycloaddition ([2+2]-PCA).[2h,i,3j–l,5g,7]

As a result of formation of 2 : 1 complexes, the cavitands CB[8] and γ-CD can promote the photochemical intermolecular [4+4]-cycloaddition, as has been demonstrated for pyridine, anthracene, and naphthalene derivatives.[2h,i,3j,k,5g,7g,8] The last-mentioned compounds are also of interest for their pronounced fluorescence, which can be affected by the complex formation with cavitands.

The final goal of our studies is to develop supramolecular machines based on these assemblies that would use light as a source of energy. To this end, the guest molecules in the pseudorotaxane inclusion complexes should be able to physically move/slide with respect to the CB[*n*] or CD molecule, which would give rise to new shuttle type supramolecular machines.

[a] *Photochemistry Center of RAS, FSRC "Crystallography and Photonics", Russian Academy of Sciences, ul. Novatorov 7A-1, Moscow 119421, Russian Federation. E-mail: spgromov@mail.ru*
[b] *N. S. Kurnakov Institute of General and Inorganic Chemistry, Russian Academy of Sciences, Leninskiy prosp. 31, Moscow 119991, Russian Federation*
[c] *N. D. Zelinskiy Institute of Organic Chemistry, Russian Academy of Sciences, Leninskiy prosp. 47, Moscow 119991, Russian Federation*
[d] *Chemistry Department, Durham University, South Road, Durham DH1 3LE, UK*
[e] *Chemistry Department, M. V. Lomonosov Moscow State University, Leninskie Gory 1-3, Moscow 119991, Russian Federation*

† Electronic supplementary information (ESI) available: ^{1}H and ^{13}C NMR spectra, UV-vis spectra, fluorescence spectra, and X-ray crystallographic data in CIF format. CCDC 1867412–1867418. For ESI and crystallographic data in CIF or other electronic format see DOI: 10.1039/c8nj04685a

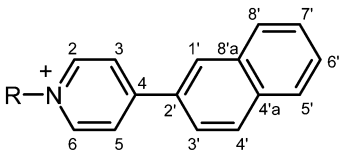

R = Me + I^- (**1**), Me + ClO_4^- (**2**), *n*-Bu + I^- (**3**), *n*-Bu + ClO_4^- (**4**), $(CH_2)_3SO_3^-$ (**5**)

Chart 1 Structure of compounds **1–5**.

We obtained the simplest supramolecular machine of this type on the basis of naphthylpyridine complex with β-CD.[4a,c] In this case, irradiation leads to reversible protonation and, as a consequence, physical motion of the guest molecule in the macrocycle cavity. A simple photocontrolled supramolecular machine was obtained in our study from the inclusion complex of a styryl dye with CB[7].[9] The considerable increase in the fluorescence lifetime of the dye was attributed to the physical motion of the dye cation deep into the cavity in the first several picoseconds, that is, the system was able to operate in the cyclic mode. A more intricate photocotrolled supramolecular machine was based on the pseudorotaxane complex of CB[8] with diquinolylethylene derivative.[10] In this case, exposure to light results in the complex formation of the unsaturated compound in the *cis*-form with CB[8]. It was found that the CB[8] cavity can accommodate two styryl dye molecules. Therefore, the [2+2]-PCA reaction between them can be induced by irradiation and, hence, a light-controlled supramolecular assembler based on CB[8] can be generated.[7f,k] A small amount of CB[8] and irradiation are sufficient for complete stereospecific conversion of the dyes to cyclobutanes. It was shown that unexcited pairs of dye molecules inside the CB[8] cavity do not conform to the topochemical requirements of the [2+2]-PCA reaction.[7f,11] The physical motion of dye molecules (translocation) towards each other over a limited distance is necessary to form a structure pre-organized for the [2+2]-PCA. The investigation and observation of the physical motions and translocations of components in the pseudorotaxane inclusion complexes of cavitands are intriguing aspects of the design of supramolecular machines.

Therefore, in this work, we studied the complex formation of quaternary 4-(2-naphthyl)pyridinium salts **1–5** (Chart 1) with cavitands, β- and γ-CD and CB[7,8], in order to determine the stoichiometry and the structure and spectral properties of inclusion complexes depending on the *N*-substituent nature in the guest molecule and the cavitand nature and cavity size.

The study was performed using ^{1}H NMR and electronic spectroscopy techniques, including spectrophotometric, fluorescence, and ^{1}H NMR titrations. X-ray diffraction study was carried out for free compounds and for two polymorphs of complex $(\mathbf{5})_2$@CB[8].

Results and discussion

Synthesis of naphthylpyridine derivatives

Quaternary salts **1–5** were prepared as depicted in Scheme 1. Quaternization of 4-(2-naphthyl)pyridine with iodomethane or 1-iodobutane afforded iodides **1** and **3**. Compounds **2** and **4**

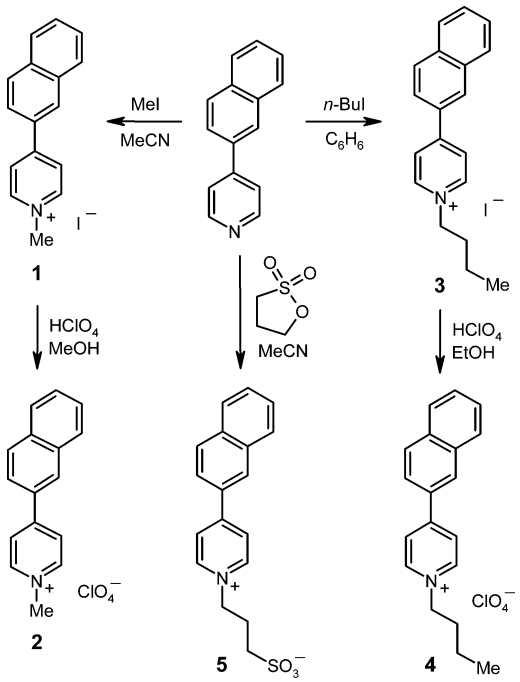

Scheme 1 Synthesis of compounds **1–5**.

were prepared by anion exchange on treatment of **1** and **3** with concentrated $HClO_4$ in alcohol. Betaine **5** was obtained by long-term keeping of a 4-(2-naphthyl)pyridine–1,3-propanesultone mixture in MeCN. Compounds **1–5** were isolated in good yields (52–94%) and analyzed by ^{1}H and ^{13}C NMR spectroscopy, spectrophotometry, and elemental analysis to confirm their structure (the ^{1}H and ^{13}C NMR spectra of compounds **1–5** are shown in Fig. S1–S10 in the ESI†).

Preparation of solid complexes

We attempted to prepare complexes of **1–5** with the cavitands in the solid state by slow evaporation of aqueous solutions of their mixtures. In most cases, the precipitates thus formed were either one of the components in a pure state or visually non-uniform polycrystalline mixtures with a non-stoichiometric component ratio (^{1}H NMR data). Only complexes $(\mathbf{1})_2$@CB[8] and $(\mathbf{5})_2$@CB[8] were obtained in this way as large yellow blocks. Colorless plate crystals with the composition 2(**5**)·γ-CD were also formed; apparently, this was either $(\mathbf{5})_2$@γ-CD or co-crystallized betaine **5** and **5**@γ-CD. The stoichiometry of solid samples was confirmed by ^{1}H NMR spectroscopy (^{1}H NMR spectra of the complexes are shown in Fig. S11–S13 in the ESI†) and elemental analysis (see Experimental section), and for $(\mathbf{5})_2$@CB[8], also by X-ray crystallography (see below).

NMR spectroscopy study

NMR spectroscopy is widely used to establish the structure and measure the stability of various supramolecular complexes in solution, in particular, to determine the mode of inclusion of the guest into the cavitand cavity and stoichiometry and stability of these complexes.[3a,b,4c,5i,7f,12] We studied mixtures of compounds **1–5** with CD and CB[7,8] using 2D NMR techniques

and ^{1}H NMR titration. According to preliminary experiments, the concentration of the hydrophobic substrates required for NMR experiment ($C_{guest} \geq 5 \times 10^{-4}$ M) could be obtained using a mixture of water with an organic solvent. We chose a D_2O–MeCN-d_3 mixture (10 : 1, v/v).

Mixing of compounds **2**, **4**, and **5** with excess CD induced small and oppositely directed shifts ($\Delta\delta_H$) of the ^{1}H NMR signals of the guest (see Fig. S14–S18 in the ESI†). For example, Fig. 1 shows changes in a mixture of **2** and β-CD, and the largest $\Delta\delta_H$ values observed for these compounds are summarized in Table 1. In all cases, the most pronounced changes ($\Delta\delta_H$ up to 0.07 ppm) were observed for signals of the pyridine ring and the 1′-H, 3′-H, and 4′-H atoms of the naphthalene residue. Apparently, these shifts are attributable to a change in the averaged rotation angle of these moieties around the C–C bond connecting them in the guest molecule after immersion into the CD cavity. Thus, irrespective of the structure of the guest *N*-substituent or the size of the CD cavity, the conjugated moiety of the guest proved to be most sensitive to complex formation, which may attest to its location mainly in the cavity.

To confirm the structures of complexes formed by naphthylpyridine derivatives and CD, we recorded the NOESY spectrum of a mixture of compound **3** and β-CD (Fig. 2). Apart from the intense intramolecular cross-peaks, the spectrum shows weaker intermolecular cross-peaks corresponding to the through-space interaction of the naphthalene protons and the 3-H and 5-H pyridine protons and the ''internal'' 3*-H and 5*-H β-CD protons. No NOE interactions were found between the *N*-butyl group protons of compound **3** and β-CD protons (see Fig. S22 in the ESI†).

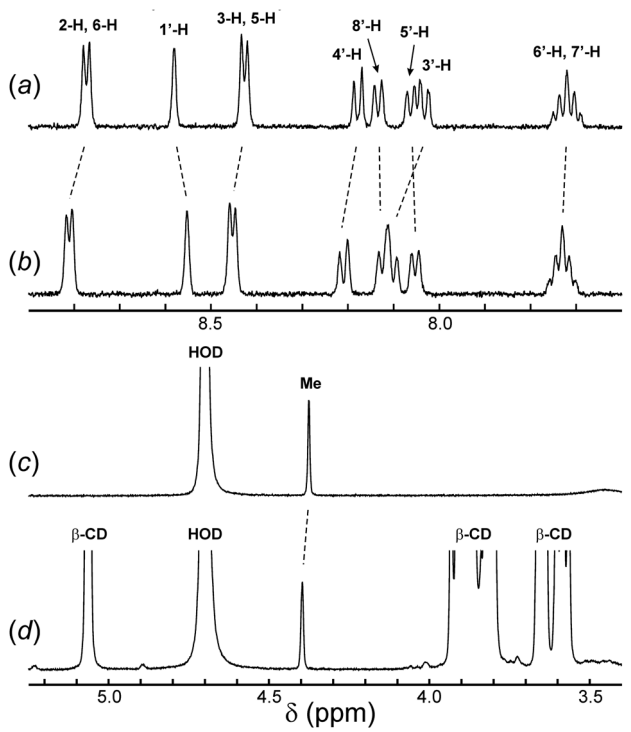

Fig. 1 ^{1}H NMR spectra ((a and b) aromatic and (c and d) aliphatic proton regions) of (a and c) compound **2** and (b and d) a 1 : 6.6 mixture of compound **2** and β-CD ($C_{\mathbf{2}} = 4.7 \times 10^{-4}$ M), D_2O–MeCN-d_3 (10 : 1, v/v), 25 °C.

Table 1 Observed maximum changes of proton chemical shifts ($\Delta\delta_{H,max}$) of compounds **1**, **2**, **4**, **5** in the presence of cavitands and stability constants of their complexes[a]

Complex	$\Delta\delta_{H,max}$[b], ppm	$\log K_{1:1}$[c]
2@β-CD	0.07	2.2
2@γ-CD	−0.04	1.7
2@CB[7]	−0.99	3.7
(**1**)$_2$@CB[8]	−1.04[e]	—[d]
4@β-CD	0.07	2.4
4@γ-CD	−0.05	2.1
4@CB[7]	−0.54	3.4
5@β-CD	0.07	2.4
5@γ-CD	−0.05	2.2
5@CB[7]	−1.07	2.7
(**5**)$_2$@CB[8]	−1.54[e]	—[d]

[a] ^{1}H NMR titration, D_2O–MeCN-d_3 (10 : 1, v/v), 25 °C. [b] $\Delta\delta_{H,max} = \delta_H$(guest–cavitand mixture) − δ_H(free guest). [c] $K_{1:1}/M^{-1}$ = [guest@cavitand]/([guest] × [cavitand]). The errors for determination of constants *K* are ±30%. [d] Low solubility of CB[8] and/or its complexes prevents carrying out the titration experiment. [e] D_2O, 25 °C.

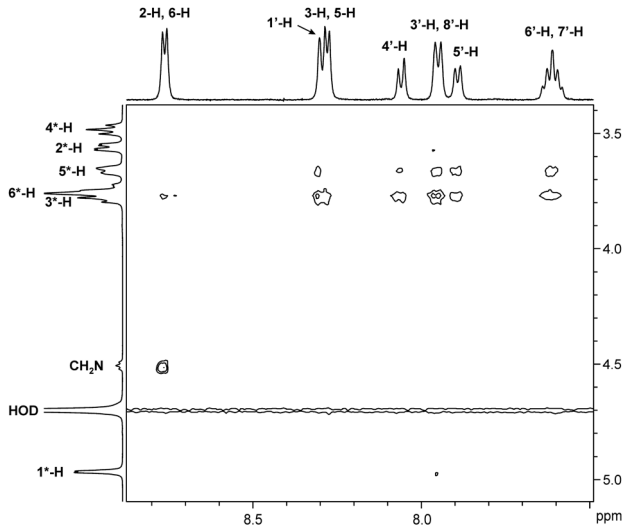

Fig. 2 Fragment of NOESY spectrum of an equimolar mixture of compound **3** and β-CD ($C_{\mathbf{3}} = C_{CD} = 6 \times 10^{-3}$ M), D_2O, 25 °C.

This leads to the conclusion that particularly the lipophilic naphthalene residue is located in the CD cavity, while the more hydrophilic pyridine ring bearing a positive charge protrudes outside of the cavity. This is in good agreement with published data on the higher CD affinity for neutral and negatively charged guests than to positively charged molecules.[3a,b,13] Fig. 3 shows two probable structures of complexes **3**@β-CD, differing in the guest position inside the unsymmetrical cavity of the cavitand. Most likely, these *anti*- and *syn*-complexes coexist in solution in equilibrium, similarly to the complexes of neutral 4-(2-naphthyl)pyridine with β-CD.[4c]

On mixing compounds **2**, **4**, or **5** with CB[7], much more pronounced changes were observed in the ^{1}H NMR spectra than in the case of CD-based mixtures.

Fig. 4 shows the changes that occur with increasing content of CB[7] in the mixture with **2**. It can be seen that the greatest

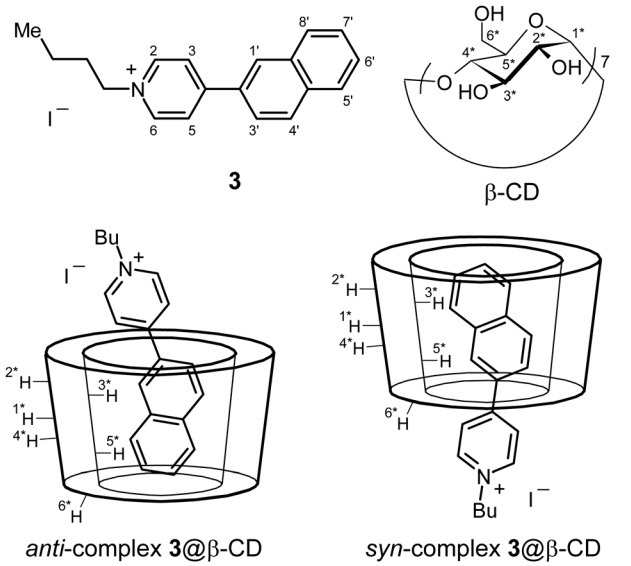

Fig. 3 Probable structure of complexes **3**@β-CD.

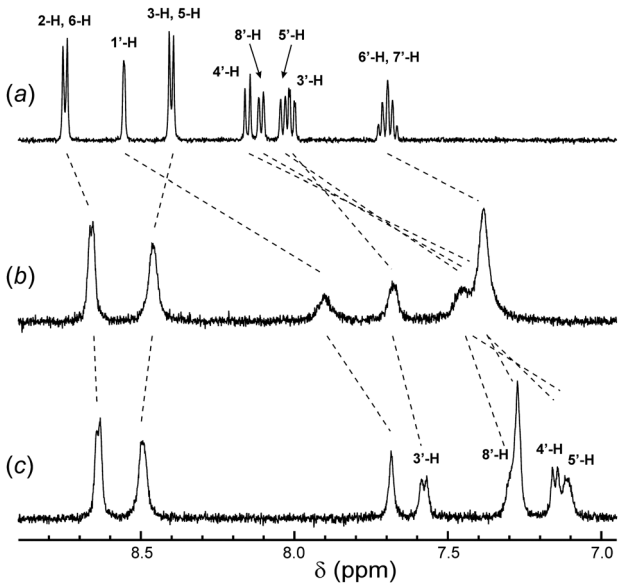

Fig. 4 ^{1}H NMR spectra (aromatic proton region) of (a) compound **2**, and (b) 1 : 1 and (c) 1 : 1.9 mixtures of compound **2** and CB[7] (C_2 = 5.7 × 10^{-4} M), D_2O–MeCN-d_3 (10 : 1, v/v), 25 °C.

upfield shifts ($\Delta\delta_H$ up to −0.99 ppm) are inherent in the signals of naphthalene protons of the guest, whereas the signals of pyridine ring protons shift to a much lesser extent and in opposite directions. The position of the *N*-methyl signal is little sensitive to the presence of CB[7] (see Fig. S21 in the ESI†). Considerable upfield shifts of proton signals indicate that these protons are shielded by the CB[7] wall, while the downfield shifts attest to proton positions in the region of deshielding of the carbonyl groups forming the portals of this cavitand. Thus, the above-listed changes clearly attest to the *endo*-structure of complex **2**@CB[7], *i.e.*, the naphthalene residue of the guest molecule is largely located inside the CB[7] cavity, while the pyridine ring protrudes outside of the cavity (Fig. 5).

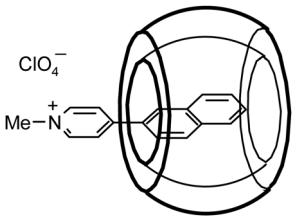

Fig. 5 Structure of *endo*-complex **2**@CB[7].

A different spectral behavior was found for compound **4** with a longer *N*-substituent (Fig. 6). The greatest upfield shifts of the butyl group proton signals and pyridine 2-H and 6-H proton signals ($\Delta\delta_H$ up to −0.54 ppm) and much smaller shifts of the naphthalene proton signals ($\Delta\delta_H$ up to −0.35 ppm) suggest that the cavitand moves along the long guest molecule, being predominantly located above the *N*-substituent (Scheme 2). Probably, the lipophilicities of the butyl group and the naphthalene residue are comparable, and the structure of inclusion complex **4**@CB[7] is crucially affected by location of the most positively charged moiety inside the cavity (*exo*-complex). This is a typical feature of the complex formation of CB[*n*], which preferably binds metal cations and positively charged organic molecules.[3e–g,k]

The complex formation of compound **5** with CB[7] resembles the complex formation observed for the **2**/CB[7] system, except for slow exchange on the ^{1}H NMR time scale (500 MHz),

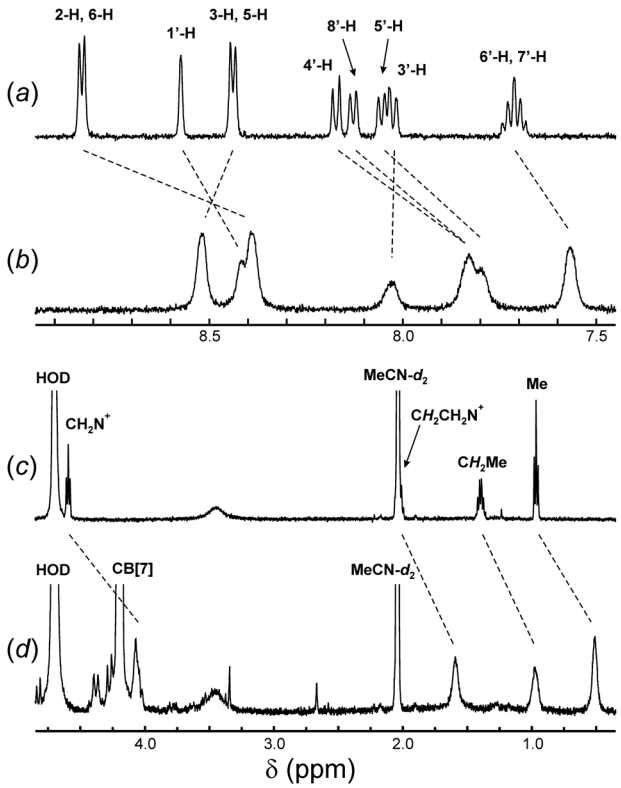

Fig. 6 ^{1}H NMR spectra ((a and b) aromatic and (c and d) aliphatic proton regions) of (a and c) compound **4** and (b and d) a 1 : 1.9 mixture of compound **4** and CB[7] (C_4 = 5.2 × 10^{-4} M), D_2O–MeCN-d_3 (10 : 1, v/v), 25 °C.

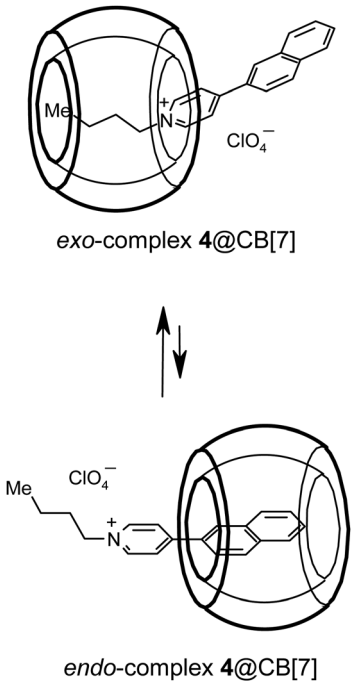

Scheme 2 Translocation of molecule **4** within CB[7] cavity.

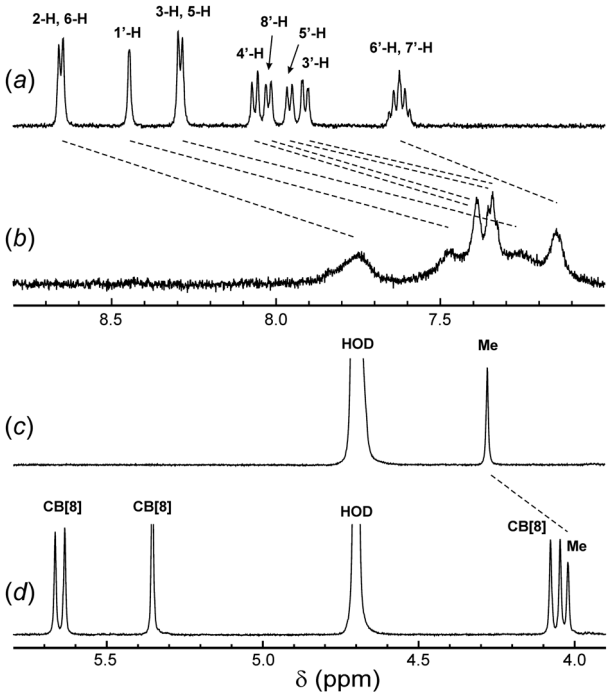

Fig. 7 ^{1}H NMR spectra ((a and b) aromatic and (c and d) aliphatic proton regions) of (a and c) compound **1** ($C_{\mathbf{1}} = 1 \times 10^{-3}$ M) and (b and d) complex $(\mathbf{1})_2$@CB[8]·6.5H_2O ($C_{complex} = 3 \times 10^{-4}$ M), D_2O, 25 °C.

which gives rise to two sets of broadened proton signals of **5** at $C_{CB[7]} < C_{\mathbf{5}}$, which correspond to the free guest and complex **5**@CB[7] (see Fig. S19 and S20 in the ESI†). Evidently, the betaine structure of molecule **5** implies a considerable decrease in the effective positive charge on the pyridine ring; therefore, the cavitand is preferably arranged above the naphthalene residue of the guest (*endo*-complex).

Detailed monitoring of the complex formation between compounds **1**–**5** and CB[8] was impossible by ^{1}H NMR spectroscopy alone, because of poor solubility of this cavitand and/or its complexes. We were still able to obtain individual complexes $(\mathbf{1})_2$@CB[8] and $(\mathbf{5})_2$@CB[8] (see above); therefore, the positions of proton signals for free and complexed **1** or **5** can be compared.

Fig. 7 shows this comparison for **1** and $(\mathbf{1})_2$@CB[8]. It can be easily seen that in the complex, the signals for all guest protons shift upfield relative to the signals of free **1**, this shift being very large, $\Delta\delta_H$ up to −1.04 ppm.

This is possible in the case where two guest cations reside in the large cavity one above another, most likely, according to the head-to-tail pattern because of the Coulomb repulsion of the likely charged pyridine residues (*endo*-complex, Fig. 8). In this case, the guest protons are shielded by not only the CB[8] wall, but also by the conjugated moiety of the second guest molecule. Apparently, the mutual positions of cations **1** inside CB[8] are not strictly fixed, *i.e.*, they can slowly (on the ^{1}H NMR time scale) move relative to each other and cavitand wall; therefore, the aromatic proton signals are highly broadened.

An interesting result was obtained from comparison of the spectra of betaine **5** and complex $(\mathbf{5})_2$@CB[8] (Fig. 9). The very poor water solubility of the latter precludes the study of the

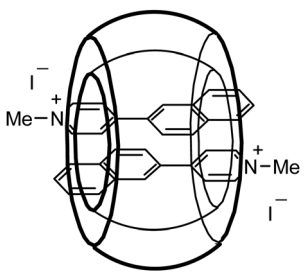

Fig. 8 Structure of *endo*-complex $(\mathbf{1})_2$@CB[8].

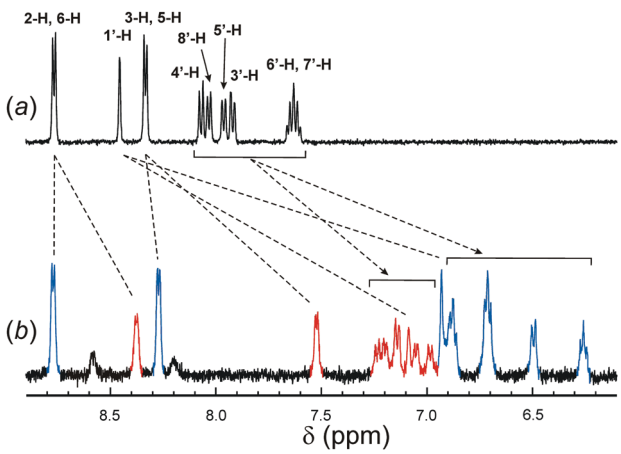

Fig. 9 ^{1}H NMR spectra (aromatic proton region) of (a) compound **5** ($C_{\mathbf{5}} = 8 \times 10^{-4}$ M) and (b) complex $(\mathbf{5})_2$@CB[8]·5H_2O (sat., $C_{complex} < 1 \times 10^{-4}$ M), D_2O, 25 °C. Blue- and red-colored signals are assigned to the *exo*- and *endo*-complexes, respectively (see Scheme 3).

complex by 2D NMR techniques; however, it is quite obvious that there are two types of complexes in solution (both of the 2(**5**):1(CB[8]) composition), which are in slow exchange on the ^{1}H NMR time scale. The aromatic proton region of the spectrum of the complex (Fig. 9b) contains two sets of clear signals marked in blue and red with a ~2 : 1 integrated intensity ratio. In the major complex, the signals of the naphthalene residue are considerably shifted upfield, whereas the signals of the pyridine ring are nearly in the same positions as in free **5**. In the case of the minor complex, the signals of all aromatic protons are shifted upfield. This means that two complexes are structurally different, in particular, in the major *exo*-complex, only the naphthalene residues of the guest molecules occur in the cavity, whereas in the minor *endo*-complex, the conjugated moieties of two molecules **5** are arranged one above another. Thus, the guest molecules physically move relative to each other inside the cavity (Scheme 3), which resembles the millstone operation. It is noteworthy that both complexes were detected by X-ray crystallography (see below).

Note that apart from the signals of the two above complexes (**5**)$_2$@CB[8], the ^{1}H NMR spectrum (see Fig. 9b) exhibits broadened signals at δ 8.2 and 8.6 ppm for pyridine protons (~10% of the integrated intensity), which apparently belong to one more type of complexes, the structure of which remains unknown.

The stability of the complexes formed by compounds **2**, **4**, and **5** with β-CD, γ-CD, and CB[7] was evaluated quantitatively by ^{1}H NMR titration. The variation of the proton signal positions for guests measured in a D_2O–MeCN-d_3 mixture (10 : 1, v/v) as a function of the concentration ratio of the components, $\Delta\delta_H - C_{cavitand}/C_{guest}$, was adequately described by the reaction model including one equilibrium:

$$\text{guest} + \text{cavitand} \overset{K_{1:1}}{\rightleftarrows} \text{guest@cavitand}, \qquad (1)$$

where $K_{1:1}/M^{-1}$ is the stability constant for 1 : 1 complex. The stability constants were calculated by the HYPNMR program;[14] the $\log K_{1:1}$ values are summarized in Table 1.

The stability of complexes for all of the guests increased in the series of cavitands: γ-CD < β-CD < CB[7], which indicates that the β-CD cavity size is more suited for binding relatively small naphthylpyridine derivatives than the γ-CD cavity size and that CB[7] has a higher affinity than CD for positively charged guests. Typically, the stability of CB[7] complexes decreases in the series of guests **2** ≈ **4** > **5**, which correlates with the decrease in the effective positive charge on the naphthylpyridinium cation on going from **2** or **4** to betaine **5**. Conversely, a decrease in the effective positive charge or increase in the hydrophobicity of the naphthylpyridinium cation leads to higher stability of CD complexes. All these trends are in good agreement with the known details of complex formation of CD and CB[*n*] with organic molecules reported in the literature.[3a,b,f,j,k,5i]

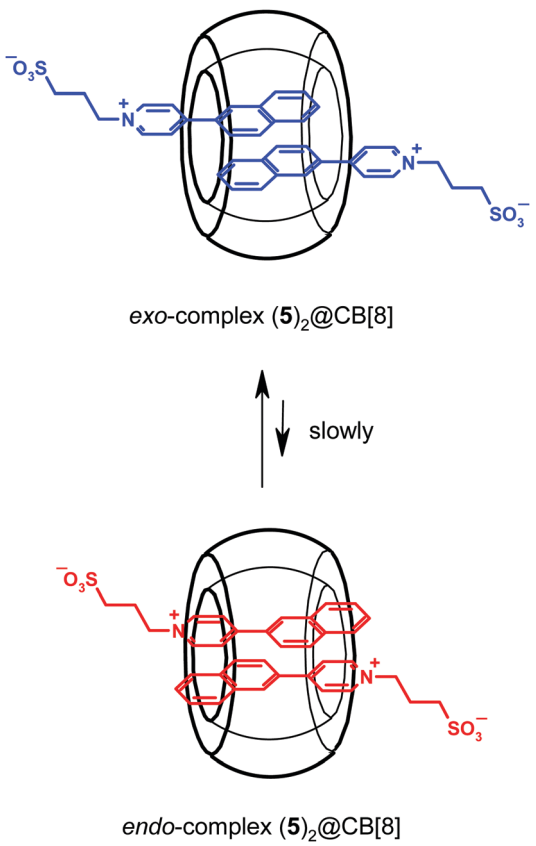

Scheme 3 Translocation of molecules **5** within CB[8] cavity.

Electronic spectroscopy studies

The measurements were conducted in aqueous solutions, as the solubility of compounds **2**, **4**, and **5** and their cavitand complexes reaches the required level of ~2 × 10^{-5} M. The spectral characteristics of free guests are summarized in Table 2 (see UV-vis and fluorescence spectra for compounds **1**, **2**, **4**, and **5** and their complexes in Fig. S23–S34 in the ESI†).

All absorption spectra exhibited two clear medium-intensity bands with peaks at 275–276 nm and 318–320 nm and a weak band with a peak at about 360 nm, which is manifested as a long-wavelength shoulder. Apparently, two former bands correspond to local electronic transitions in the pyridine and naphthalene residues, respectively, while the band at ~360 nm is due to electronic transition of the whole chromophore. Moderate intensity of this band (ε_{max} ≈ 6000 M^{-1} cm^{-1}) attests to relatively low degree of conjugation between the pyridine and naphthalene residues in compounds **1**–**5**, probably, because of their rotation around the linking C–C bond caused by steric contacts between the protons in the *ortho*-positions to this bond.

All compounds under study produce intense fluorescence in the 400–650 nm range. The fluorescence spectra have a single-band nearly symmetric shape with peaks at 472–478 nm. From this, it can be concluded that fluorescence occurs from the excited state with the highest degree of conjugation between the aromatic parts of the naphthylpyridinium cation, which is possible only for a planar conformation of this cation.

The addition of excess β- or γ-CD to solutions of compounds **2**, **4**, and **5** induces minor changes in the absorption spectra and weak fluorescence quenching, these changes being least pronounced in the case of γ-CD (see Fig. S25–S30 in the ESI†).

Table 2 Spectral characteristics of compounds **2**, **4**, **5** and their complexes with cavitands and stability constants[a]

Compound	λ^{abs}_{max}/nm (ε_{max}/M^{-1} cm^{-1})	$\Delta\lambda^{abs}_{max}$[b]/nm	λ^{f}_{max}/nm	$\Delta\lambda^{f}_{max}$[b]/nm	Q[c]	log $K_{1:1}$[d]	log $K_{1:2}$[d]	log $K_{2:1}$[d]
2	318 (19 300), 275 (25 700)		474					
2@β-CD	318 (18 600), 275 (26 000)	0, 0	477	3	0.94	3.2 (2.7[e])		
2@γ-CD	317 (18 700), 275 (27 000)	−1, 0	474	0	0.50	2.0 (<2[e])		
2@CB[7]	329 (17 300), 280 (15 000)	11, 5	465	−9	1.17	>6 (~7.1[e])		
2@(CB[7])$_2$	328 (17 600), 280 (15 300)	10, 5	463	−11	1.26		>6 (6.1[e])	
2@CB[8]	324 (13 300), 281 (13 300)	6, 6	484	10	0.66	>6 (6.7[e])		
(**2**)$_2$@CB[8]	324 (12 800[f]), 280 (128 00[f])	6, 5	497	23	0.57[f]			>6 (6.4[e])
4	319 (21 100), 275 (27 100)		472					
4@β-CD	319 (20 700), 276 (26 700)	0, 1	496	24	0.83	4.2 (2.7[e])		
4@γ-CD	318 (21 100), 276 (28 200)	−1, 1	474	2	0.75	2.2 (~2[e])		
4@CB[7]	324 (19 000), 277 (19 700)	5, 2	462	−10	1.22	>6 (>7[e])		
4@(CB[7])$_2$	324 (20 300), 277 (20 900)	5, 2	463	−9	1.40		>6 (6.5[e])	
4@CB[8]	328 (21 400), 281 (19 000)	10, 6	445	−27	1.53	>6 (>7[e])		
(**4**)$_2$@CB[8]	326 (13 400[f]), 286 (12 100[f])	8, 11	452	−20	0.85[f]			>6 (>7[e])
5	320 (22 800), 276 (28 300)		478					
5@β-CD	318 (21 300), 277 (32 600)	−2, 1	489	11	0.89	2.6 (2.8[e])		
5@γ-CD	319 (22 400), 276 (30 900)	−1, 0	480	2	0.90	1.9 (<2[e])		
5@CB[7]	332 (20 800), 281 (16 200)	12, 5	464	−14	1.22	>6 (>7[e])		
5@(CB[7])$_2$	331 (21 000), 281 (17 300)	11, 5	463	−15	1.31		>6 (6.5[e])	
5@CB[8]	330 (14 300), 284 (11 400)	10, 8	522	44	0.61	>6 (>7[e])		
(**5**)$_2$@CB[8]	331 (14 100[f]), 287 (11 300[f])	11, 11	511	33	0.65[f]			>6 (6.7[e])

[a] Spectrophotometric titration, water, ambient temperature. [b] $\Delta\lambda_{max} = \lambda_{max}$(complex) − λ_{max}(free guest). [c] The integrated fluorescence intensity ratio for the complex and the free guest. [d] $K_{1:1}$/M^{-1} = [guest@cavitand]/([guest] × [cavitand]), $K_{1:2}$/M^{-1} = [guest@(CB[7])$_2$]/([guest@CB[7]] × [CB[7]]), $K_{2:1}$/M^{-1} = [(guest)$_2$@CB[8]]/([guest@CB[8]] × [guest]). The determination errors of the stability constants are ±30%. [e] Fluorescence titration, water, ambient temperature. The fluorescence was excited at the wavelength at which the extinction values for the free naphthylpyridine derivative and its complexes differ the least (from spectrophotometry data). [f] Per molecule of naphthylpyridine derivative.

This attests to slight influence of the arrangement of the naphthylpyridine derivative in the CD cavity on the guest conformation and local solvation and provides indirect evidence for the relatively low stability of the resulting complexes.

In the presence of excess CB[*n*], a more substantial changes take place in the absorption and fluorescence spectra of compounds **2**, **4**, and **5** than in the CD systems (see Fig. S31–S34 in the ESI†). As an example, Fig. 10 shows typical changes occurring in the absorption and fluorescence spectra of **5** with increasing concentration of CB[7]. Upon the complex formation, the absorption spectrum of the guest entirely shifts to the red region (by ~10 nm), with the intensity of local electronic transition bands being decreased. The fluorescence of the complexes is somewhat enhanced, with the maximum shifting to the blue region by 10–15 nm. This is a typical behavior for the formation of complexes between CB[*n*] (*n* = 6, 7) and donor–acceptor type guest molecules (see, for example, similar changes for styryl dyes[5h,i,15]). This is attributed to the change in the polarity of the chromogen local environment upon migration of the guest from the aqueous medium to the CB[*n*] cavity. In the case of styryl dye, up to 25-fold fluorescence enhancement was observed in the complexes with CB[7].[5h] For naphthylpyridine derivatives, the enhancement was not so strong, evidently, due to efficient fluorescence of the free compounds. For example, the fluorescence quantum yield of the 4-(2-naphthyl)pyridinium cation formed upon the photoinduced protonation of neutral 4-(2-naphthyl)pyridine in water is 0.90.[4a]

The changes in the absorption spectra of compounds **2**, **4**, and **5** upon the addition of excess CB[8] are qualitatively the same as for analogous systems based on CB[7]. However, the changes in the fluorescence spectra of **2**, **4**, and **5** in the presence

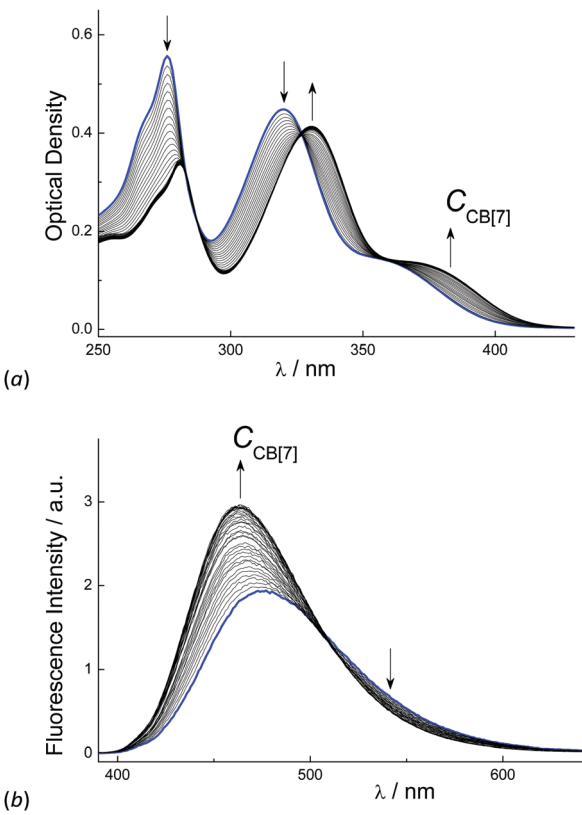

Fig. 10 (a) Absorption and (b) fluorescence spectra of compound **5** ($C_{\mathbf{5}}$ = 2 × 10^{-5} M for absorption, $C_{\mathbf{5}}$ = 1 × 10^{-6} M for fluorescence) measured for different concentrations of CB[7] (C_{CB} varies from 0 to 1.9 × 10^{-4} M for absorption, C_{CB} varies from 0 to 9.1 × 10^{-6} M for fluorescence), water, ambient temperature. The fluorescence was excited by light at 359 nm. Blue curves are the spectra of free **5**.

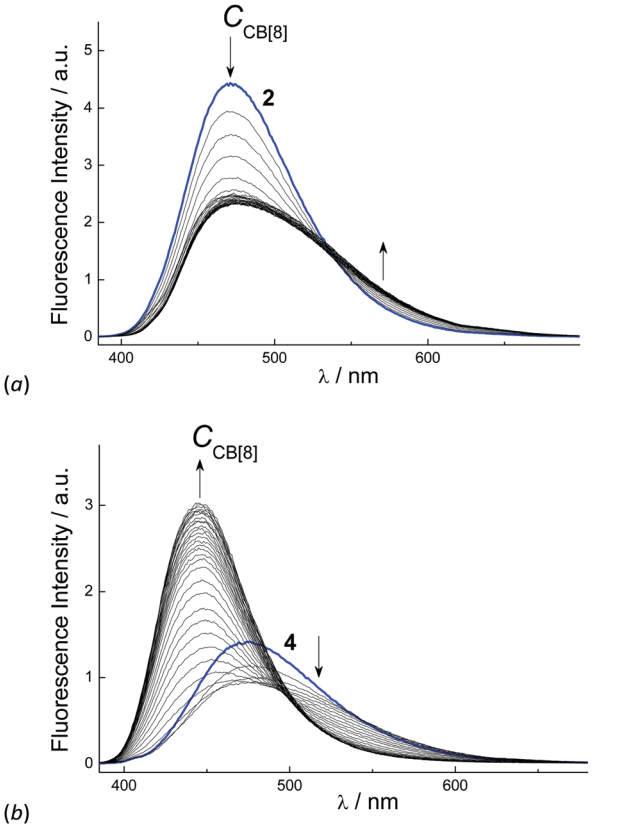

Fig. 11 Fluorescence spectra of (a) compound **2** and (b) compound **4** (C_{guest} = 1 × 10^{-6} M) measured for different concentrations of CB[8] (C_{CB} varies from 0 to 9.1 × 10^{-6} M), water, ambient temperature. The fluorescence was excited by light at 367 nm (for **2**) and 356 nm (for **4**). Blue curves are the spectra of free guests.

of CB[8] are different (Fig. 11). The gradual increase in the cavitand concentration in solutions of compounds **2** and **5** results first in a noticeable fluorescence quenching and then in a slight increase in the fluorescence intensity (in the case of **5**, the fluorescence peak markedly shifts to the red region (see Fig. S34 in the ESI†)). Conversely, increasing the content of CB[8] in the mixture with compound **4** results first in a minor fluorescence quenching followed by considerable fluorescence enhancement and a blue shift of the maximum. These spectral differences attest to the presence of two or more complex formation equilibria involving this host and different structures of complexes.

The variation of the absorption and fluorescence spectra of compounds **2**, **4**, and **5** with the β-CD and γ-CD concentrations was adequately described by equilibrium (1). In the case of complex formation with CB[7], it was also necessary to include the following equilibrium:

$$\text{guest@CB[7]} + \text{CB[7]} \overset{K_{1:2}}{\rightleftarrows} \text{guest@(CB[7])}_2, \qquad (2)$$

where $K_{1:2}/M^{-1}$ is the stability constant of the 1 : 2 complex. In the case of CB[8], inclusion of equilibria (1) and (3) was beneficial:

$$\text{guest@CB[8]} + \text{guest} \overset{K_{2:1}}{\rightleftarrows} \text{guest}_2\text{@CB[8]}, \qquad (3)$$

where $K_{2:1}/M^{-1}$ is the stability constant of the 2 : 1 complex. The concentration dependences of the absorption spectra were analyzed and the stability constants of the complexes were calculated by the HypSpec program included in the Hyperquad package.[16] The obtained data on the spectral properties and stability of the complexes are summarized in Table 2.

The stability constants of all 1 : 1 inclusion complexes in pure water exceed the values measured in a D_2O–MeCN-d_3 mixture (10 : 1, v/v) (*cf.* data of Tables 1 and 2). Previously we showed, in relation to the complex formation of styryl heterocycles with β-CD, that increasing MeCN content in water–acetonitrile mixtures leads to a considerable decrease in $\log K_{1:1}$.[5i] Obviously, the same trend holds for the complex formation of naphthylpyridine derivatives with the cavitands.

The accuracy of measurements of the stability constants of the CD-based complexes is reduced due to low spectral changes that accompany fluorescence and especially spectrophotometric titrations. This may account for the differences between the $\log K_{1:1}$ values obtained by the two mentioned methods. Generally, the detected trends of variation of $\log K_{1:1}$ as a function of guest structure and cavitand size are the same as found by ^{1}H NMR titration.

The stability of 1 : 1 complexes of **2**, **4**, and **5** with CB[7] in water proved to be very high, exceeding the values obtained in a water–acetonitrile mixture by more than three orders of magnitude (see Table 1). This is above the upper limit of applicability of the spectrophotometric titration technique ($\log K \leq 6$ [M^{-1}]). Furthermore, in the processing of titration data, it was necessary to include also trimolecular complexes guest@$(CB[7])_2$, which can be formed upon threading of a second cavitand molecule onto the long guest molecule which is already contained in the guest@CB[7] complex. The stability of trimolecular complexes also exceeded $\log K_{1:2} > 6$ [M^{-1}]. The fluorescence titration data indicate the formation of highly stable 1 : 1 and 1 : 2 complexes. The upper limit of applicability of fluorescence titration is $\log K \leq 7$ [M^{-1}]; therefore, we were able to roughly evaluate the stability of **2**@CB[7] as $\log K_{1:1} \approx 7.1$ [M^{-1}], while the 1 : 1 complexes of **4** and **5** were even more stable. The stability of trimolecular complexes of **2**, **4**, and **5** with CB[7] derived from the fluorescence titration data is $\log K_{1:2}$ = 6.1–6.5 [M^{-1}].

The absorption and fluorescence spectra of guest@CB[7] and guest@$(CB[7])_2$ are very similar (see Fig. S31–S34 in the ESI†), which introduces an additional error for calculation of $\log K_{1:1}$ and $\log K_{1:2}$.

According to electronic spectroscopy data in water, all of the naphthylpyridine derivatives are complexed with CB[8] to give 1 : 1 and 2 : 1 complexes, which are very stable ($\log K_{1:1} \geq 6.7$ [M^{-1}], $\log K_{2:1} \geq 6.4$ [M^{-1}]). As in the case of CB[7] complexes, the stability of CB[8] complexes increases in the series **2** < **5** ≤ **4**. Apparently, a longer *N*-substituent enhances the guest affinity for the lipophilic cavity of the cavitand.

An interesting difference between the absorption spectra of complexes formed by **2**, **5**, and **4** with CB[8] deserves mention. The evaluated spectra of **2**@CB[8] and $(\mathbf{2})_2$@CB[8] differ little from each other (Fig. 12a) (the situation is similar for the complexes of **5** (see Fig. S34 in the ESI†)). Conversely, the spectra of

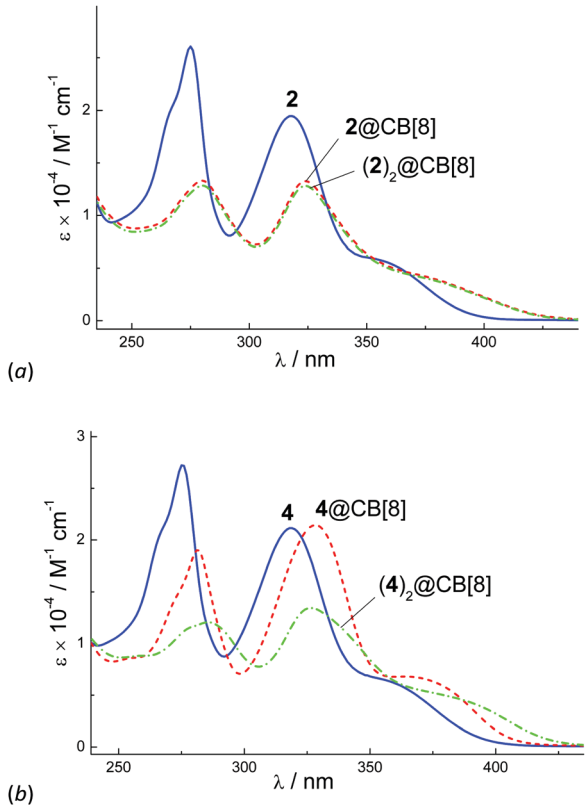

Fig. 12 Absorption spectra of (a) compound **2** and (b) compound **4** and respective evaluated spectra of their complexes with CB[8] (per molecule of naphthylpyridine derivative), water, ambient temperature.

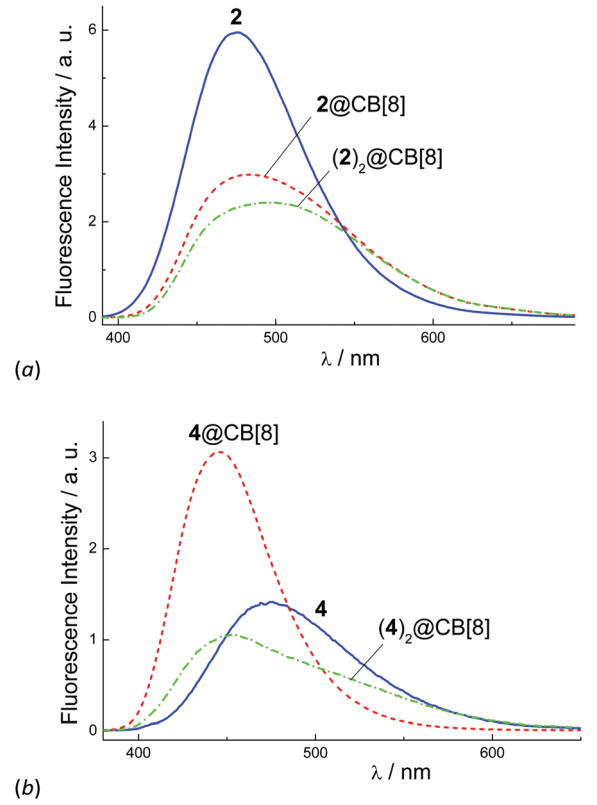

Fig. 13 Fluorescence spectra of (a) compound **2** and (b) compound **4** (C_{guest} = 1 × 10^{-6} M) and respective evaluated spectra of their complexes with CB[8] (per molecule of naphthylpyridine derivative), water, ambient temperature. The fluorescence was excited by light at 367 nm (for **2**) and 356 nm (for **4**).

bi- and trimolecular complexes of **4** differ considerably (Fig. 12b). It follows from ^{1}H NMR spectroscopy (see Fig. 8 and Scheme 3) and X-ray crystallography data (see below) that the naphthalene moiety in (**1**)$_2$@CB[8] and (**5**)$_2$@CB[8] is located inside the cavity. Apparently, complex **2**@CB[8] has a structure similar to that of *endo*-complex **2**@CB[7] (see Fig. 5), *i.e.*, the naphthalene moiety is also inside CB[8]. The absorption spectrum of (**4**)$_2$@CB[8] has a similar form and, hence, in this complex, too, the naphthalene residues of two molecules **4** are located inside the cavity. The considerable difference between the spectra of **4**@CB[8] and (**4**)$_2$@CB[8] implies that in the former case, the cavity is occupied by the butylpyridinium group (like in *exo*-complex **4**@CB[7] shown in Scheme 2).

Fig. 13 shows the fluorescence spectra of compounds **2** and **4** and evaluated fluorescence spectra of their 1 : 1 and 2 : 1 complexes with CB[8]. If the naphthalene residue of these compounds is located inside the cavity, fluorescence quenching is observed and, conversely, if the *N*-alkylpyridinium residue is in the cavity, fluorescence is enhanced. Thus, the electronic spectra of quaternary 4-(2-naphthyl)pyridinium salts provide conclusions about the structure of the inclusion complexes they form with CB[8].

X-ray crystallography

The structure of compound **2** was determined in our previous study.[4c] Compounds **1** and **3** (as two solvation-free polymorphs, **3**(1) and **3**(2)) and **5** (as two polymorphs) and complex (**5**)$_2$@CB[8] (as two polymorphs) were obtained as single crystals and studied by X-ray diffraction. The structures of these compounds are shown in Fig. 14–16.

The structures of **1**·C_6H_6, **3**(1), **5**·0.5C_6H_6·2H_2O, and **5**·4H_2O were solved with a rather high accuracy. The structures of **1**·C_6H_6 and **3**(1) were found to contain two independent molecules of naphthylpyridine derivatives. One independent molecule in structure **1**·C_6H_6 is disordered over two positions with the 0.67 : 0.33 occupancy ratio. The organic cation and iodide anion in **3**(2) proved to be substantially disordered over a series of close positions, which considerably reduces the quality of the X-ray experiment. This disorder is caused by the less close molecular packing of **3**(2) compared with **3**(1), which is obvious from the calculated densities of these crystals (1.377 and 1.522 g cm^{-3}, respectively). Therefore, for structure **3**(2), we discuss only the general geometric characteristic of the molecule. The bond length distribution in the accurately solved structures is typical of the naphthalene and quaternized pyridine residues. The length of the C–C bonds connecting these residues are 1.470(3)–1.516(16) Å [in compound **2**, the length of this bond is 1.485(2) Å (see lit.[4c])]. In all structures, the aromatic moieties of compounds **1**, **3**, and **5** exist as a nearly planar or weakly twisted conformation, which is most suitable for effective conjugation over the whole

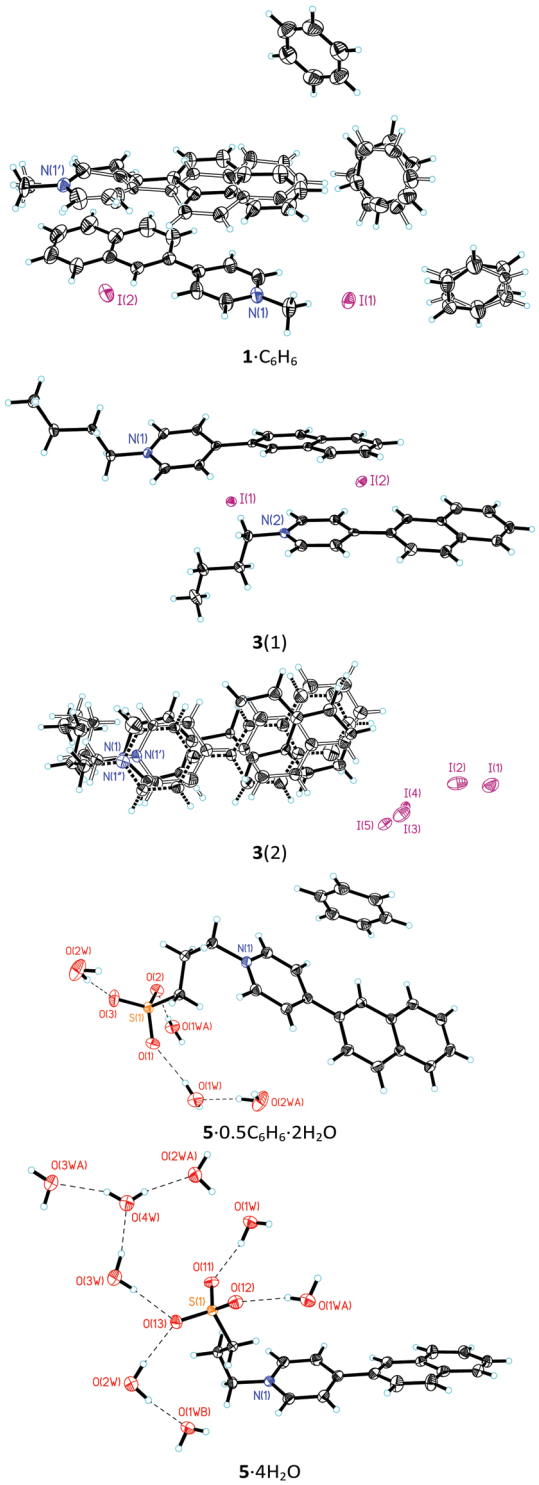

Fig. 14 Structures $\mathbf{1}\cdot C_6H_6$ (two independent molecules **1**, one of which is disordered), **3**(1) (two independent molecules), **3**(2) (all components of the crystal cell are disordered), $\mathbf{5}\cdot 0.5C_6H_6\cdot 2H_2O$, and $\mathbf{5}\cdot 4H_2O$. Thermal ellipsoids are drawn at the 20% (for **3**(2)), 40% (for $\mathbf{1}\cdot C_6H_6$), and 50% (for the other structures) probability level. Hydrogen bonds are drawn with dash lines. Additional letters "A" and "B" indicate that atoms belong to symmetrically related sites.

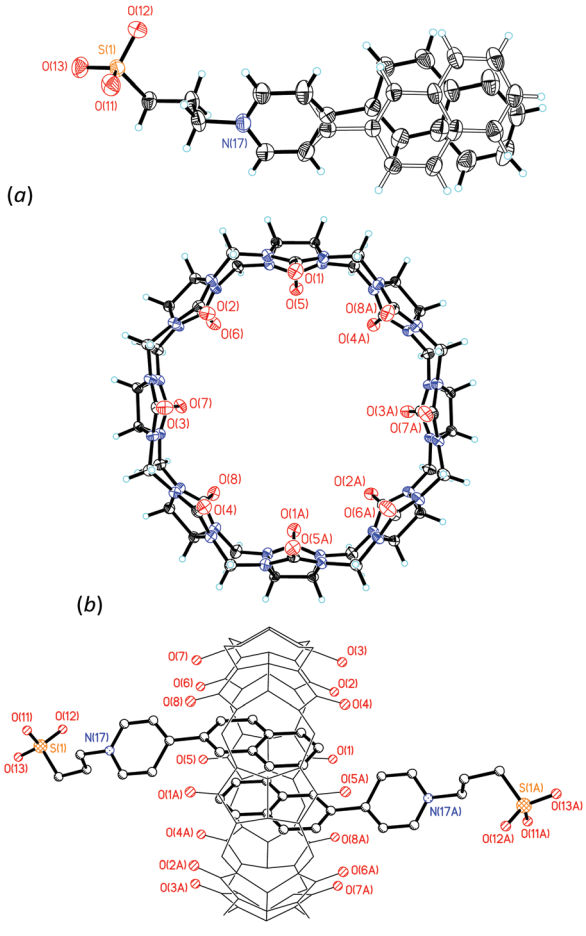

Fig. 15 Structure of *exo*-complex $(\mathbf{5})_2$@CB[8]·$28.5H_2O$ (first polymorph) and its components: (a) disordered molecule **5**, (b) molecule CB[8], (c) side projection of complex $(\mathbf{5})_2$@CB[8] (the disorder of molecules **5**, hydrogen atoms, and water molecules of solvation are omitted for clarity). Thermal ellipsoids are drawn at the 30% probability level. Additional letters "A" indicate that atoms belong to symmetrically related sites.

chromophore: the dihedral angles between the planes of the pyridine and naphthalene residues are 8.5°, 4.1°, and 13.5° (for $\mathbf{1}\cdot C_6H_6$); 24.6° and 7.3° (for **3**(1)); 3.2°, 6.6°, and 5.3° (for **3**(2)); 14.5° (for $\mathbf{5}\cdot 0.5C_6H_6\cdot 2H_2O$); and 18.2° (for $\mathbf{5}\cdot 4H_2O$) (*cf.* 3.9° for **2**[4c]). Thus, rotation of the pyridine and naphthalene residues around the connecting bond in the quaternary 4-(2-naphthyl)pyridine salts is, in principle, possible, but over a relatively narrow range.

The structures of betaine **5** additionally include 2 or 4 solvation water molecules. All three oxygen atoms of the SO_3^- group form medium-strength hydrogen bonds with these water molecules or their symmetrical equivalents; the SO···H–O bond lengths are 1.93(3)–2.04(2) Å, while the corresponding angles at the hydrogen atoms are 162(2)°–173(2)°. The water molecules are also hydrogen-bonded (see Fig. 14). In $\mathbf{5}\cdot 0.5C_6H_6\cdot 2H_2O$, the O(2WA)–H···O(1W) bond length is 1.93(3) Å and the angle is 173(2)°; in $\mathbf{5}\cdot 4H_2O$, the lengths of the O(2W)–H···O(1WB), O(3W)–H···O(4W), O(4W)–H···O(3WA), and O(4W)–H···O(2WA) bonds are in the 1.86(4)–2.04(3) Å range and the angles are in the 158(3)°–166(3)° range. Thus, the crystals of compound **5** contain infinite chains or two-dimensional layers of hydrogen-bonded

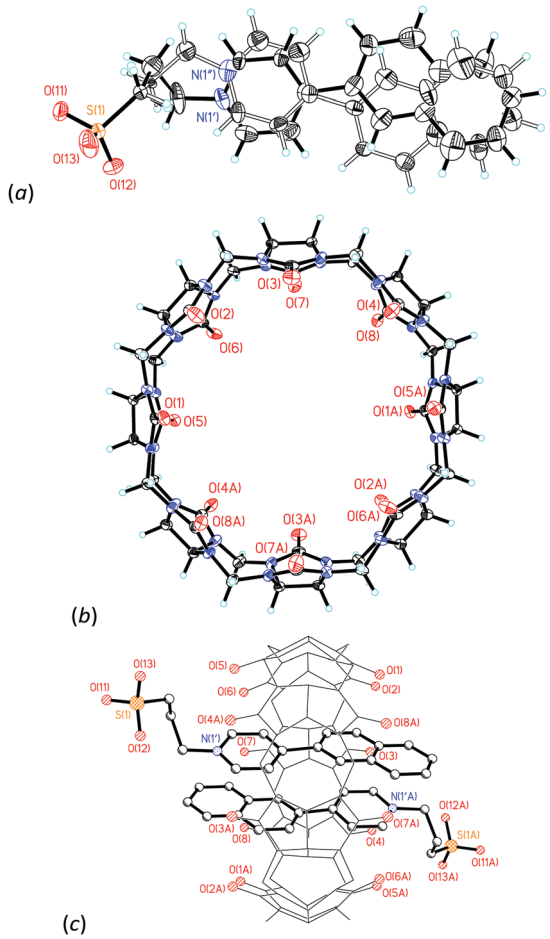

Fig. 16 Structure of *endo*-complex $(\mathbf{5})_2$@CB[8]·15.7H_2O (second polymorph) and its components: (a) disordered molecule **5**, (b) molecule CB[8], (c) a side projection of complex $(\mathbf{5})_2$@CB[8] (the disorder of molecules **5**, hydrogen atoms, and water molecules of solvation are omitted for clarity). Thermal ellipsoids are drawn at the 30% probability level. Additional letters "A" indicate that atoms belong to symmetrically related sites.

sulfonate groups and water molecules. The presence of solvation water in compound **5** is confirmed by elemental analysis (see Experimental section); furthermore, this water cannot be removed by drying the sample at 80 °C in a vacuum. This behavior is typical of such compounds because of the high proneness of the SO_3^- group to form hydrates.

In the co-crystallized compound **5** and CB[8], crystals of two polymorphs of complex $(\mathbf{5})_2$@CB[8] (as yellow prisms) were detected, differing in the mutual positions of complexes and the number of solvation water molecules.

Conducting the X-ray diffraction experiment for $(\mathbf{5})_2$@CB[8]·28.5H_2O (first polymorph) was faced with difficulties. On cooling to 170 K, the crystal was soon covered with cracks (*i.e.*, fractured), which precluded structure solution. Apparently, deep cooling induces a phase transition that changes the inner structure of the crystal. At room temperature, the solvation water soon evaporated, which also led to destruction of the crystal. It was found experimentally that only cooling to 240 K allows one to preserve the crystal for a long period of time sufficient for an X-ray diffraction experiment. For this reason and because of disorder of molecule **5** and solvation shell, the structure of the complex was determined with a moderate accuracy; however, it can be stated with confidence that the found structural motif and general geometry of the complex were sufficiently correct for discussing the relative positions of components.

In $(\mathbf{5})_2$@CB[8]·28.5H_2O, the CB[8] molecule is located at the center of symmetry of the unit cell and is round-shaped: the distances between the opposing oxygen atoms are close to each other in each portal (9.81–10.40 Å). In molecule **5**, the naphthalene residue proved to be disordered with nearly equal position occupancy (see Fig. 15a). The chromophore moiety in both conformers of **5** is twisted to higher extent than those in free **1**, **2**, **3**, and **5**: the dihedral angles between the pyridine and naphthalene planes are 37.8° and 38.5°. This structure was found to contain 34 solvation water molecules per structural unit of the complex; some water molecules are disordered or have incomplete position occupancy. The sulfonate group of molecule **5** forms apparently three relatively strong hydrogen bonds with the water molecules H_2O(1W), H_2O(3W), and H_2O(5W), with the $H_2O\cdots OS$ distances being about 2.7–2.8 Å. In the crystal lattice, the complexes are surrounded from all sides by numerous water molecules and barely touch one another. Actually, we are dealing with a structured solid aqueous solution the components of which are weakly attached to one another and are held only by hydrogen bonds that arise between water molecules and sulfonate groups.

The first polymorph of $(\mathbf{5})_2$@CB[8] corresponds to the *exo*-complex, which predominates in solution and has been detected by ^{1}H NMR spectroscopy (see above). The positions of the key components of the crystal lattice of $(\mathbf{5})_2$@CB[8]·28.5H_2O are shown in Fig. 15c. The CB[8] cavity accommodates a centrosymmetric head-to-tail dimeric pair of molecules **5**. Only the naphthalene residues of each guest molecule are located directly in the cavity, while two $Py^+(CH_2)_3SO_3^-$ groups protrude on both sides of the torus-shaped cavitand portals. Probably, this arrangement of the parts of molecule **5** with respect to the CB[8] wall is caused by the fact that interaction of the hydrophobic CB[8] cavity with the annelated aromatic system is more favorable than with the positively charged pyridinium ring, the charge of which is reduced by the proximate anionic group.

The crystals of the second polymorph, $(\mathbf{5})_2$@CB[8]·15.7H_2O, proved to be more stable without a solvent; they were found in a dry co-crystallized sample among the crystals of the first polymorph destroyed by weathering. As in the case of the first polymorph, the disordered position of molecule **5** and, especially, the solvation shell accounts for the moderate accuracy of this X-ray diffraction experiment; however, in this case, too, the structural motif and the general geometry were determined quite correctly.

As in the first polymorph, in $(\mathbf{5})_2$@CB[8]·15.7H_2O, the CB[8] molecule is located at the crystal center of symmetry and is also round-shaped: the distances between the opposing oxygen atoms on each portal are 9.85–10.44 Å. Except for the terminal $CH_2SO_3^-$ moiety, molecule **5** is disordered over two positions with the 0.52 : 0.48 occupancy ratio (see Fig. 16a). The chromophore

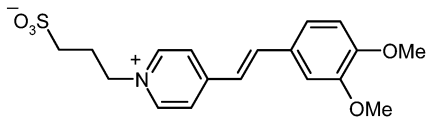

6

Chart 2 Structure of dye **6**.

moiety in both conformers of **5** is rotated slightly, the dihedral angles between the pyridine and naphthalene planes being 8.2° and 11.1°. All 22 independent water molecules in this structure have incomplete site occupancy, which is indicative of the substantial disorder of the solvation shell. The sulfonate group of molecule **5** is likely to form four hydrogen bonds with the water molecules H_2O(3W), H_2O(4W), H_2O(12W), and H_2O(21W), with the $H_2O\cdots OS$ distances being approximately 2.7–2.8 Å. In the crystal lattice, the complexes contact *via* the van der Waals interactions, which distinguishes this polymorph from the former one and probably accounts for its higher stability against weathering.

The second polymorph of $(\mathbf{5})_2$@CB[8] corresponds to the minor *endo*-complex, which is also present in solutions according to ^{1}H NMR data. The positions of the principal crystal lattice components for $(\mathbf{5})_2$@CB[8]·15.7H_2O are shown in Fig. 16c. The cavity of the cavitand accommodates a centrosymmetric head-to-tail dimeric pair of molecules **5**, with their conjugated moieties being nearly parallel, separated by 3.2–3.6 Å distances, and completely projected one onto the other. This implies a strong stacking interaction between molecules **5** within the CB[8] cavity. The CB[8] molecule is located above the central region of the conjugated moieties of the dimer of **5**, while their terminal regions protrude beyond the cavity. Thus, the second polymorph of $(\mathbf{5})_2$@CB[8] is a pseudo-rotaxane sandwich structure. Previously, we found a similar structure[7f] for the crystalline complex of the betaine styryl dye **6** (see Chart 2) with CB[8] ($(\mathbf{6})_2$@CB[8]), in which the vinylpyridinium moieties of the dye molecules were located inside the cavity.

Conclusions

Thus, the synthesis of the quaternary 4-(2-naphthyl)pyridinium salts with different *N*-substituents was developed and the compounds were studied by X-ray crystallography. The complex formation of these compounds with CD and CB[*n*] in aqueous solutions was studied by electronic and ^{1}H NMR spectroscopy. It was found that the stability of 1 : 1 inclusion complexes for all of the naphthylpyridine derivatives tends to increase in the series γ-CD < β-CD ≪ CB[7] ≈ CB[8]. Highly stable complexes, guest@$(CB[7])_2$ and $(guest)_2$@CB[8], were found to form due to the sufficient length of guest molecules and large size of CB[8] cavity. In the CD complexes, the cavity preferably accommodates the hydrophobic naphthalene residue of the guest, whereas in the case of CB[*n*], the structure of complexes is dictated by the length and the nature of the *N*-substituent in the naphthylpyridine derivative. The CB[7] and CB[8] cavities preferably contain either the naphthalene residue or the whole conjugated part of the guest molecule having a methyl or sulfonatopropyl group. In the case of long hydrophobic *N*-butyl substituent in the pyridine residue, the guest tends to immerse this group into the CB[7] cavity. It was found that the structure of CB[8]-based 1 : 1 complexes can also be determined by electronic spectroscopy. Physical motion of the long guest molecules in the CB[7,8] cavities was found. For the 2 : 1 complex formed by betaine type naphthylpyridine derivative with CB[8], this translocation, resembling the millstone operation, is not only observed for the first time by NMR spectroscopy, but is also confirmed by X-ray crystallography. The detected trends of the translocations in the inclusion complexes of the cavitands can be used to design supramolecular devices and machines, in particular, supramolecular assemblers, and to develop information recording and storage devices at the molecular level.

Experimental section

General

The melting points were measured using a Mel-Temp II apparatus in a capillary and are uncorrected. The ^{1}H and ^{13}C NMR spectra were recorded on a Bruker DRX500 instrument in DMSO-d_6 and D_2O using the solvent as the internal reference (δ_H 2.50 and 4.70 ppm, respectively; δ_C 39.43 ppm for DMSO-d_6); *J* values are given in Hz. 2D NOESY spectra and ^{1}H–^{13}C correlation spectra (HSQC and HMBC) were used to assign the proton and carbon signals (see Chart 1 for atom numbering in compounds **1–5**); the mixing time in the NOESY experiments was 300 μs. Absorption and emission spectra were recorded on a Cary 4000 spectrophotometer (Agilent) and an RF5301PC spectrofluorimeter (Shimadzu) in the range of 200–600 nm and 360–710 nm, respectively, with an increment of 1 nm in deionized water (HPLC grade, Aldrich) at ambient temperature using 1 cm quartz cells. Elemental analyses were performed at the microanalytical laboratory of the A. N. Nesmeyanov Institute of Organoelement Compounds (Moscow, Russian Federation); the samples for elemental analysis were dried *in vacuo* at 80 °C. Compounds **2** and **4** containing perchlorate anions are non-explosive.

Preparations

MeI, 1-iodobutane, 1,3-propanesultone, $HClO_4$ (70%, aq.), β-CD·9.5H_2O, γ-CD·4.5H_2O, CB[7]·13H_2O, and CB[8]·14H_2O (Sigma-Aldrich) were used as received. 4-(2-Naphthyl)pyridine was obtained according to a published procedure.[17]

1-Methyl-4-(2-naphthyl)pyridinium iodide (1). A solution of a mixture of 4-(2-naphthyl)pyridine (60.2 mg, 0.29 mmol) and MeI (55 μdm^3, 0.88 mmol) in MeCN (1 cm^3) was kept in the dark at ambient temperature for 24 h. The solvent was evaporated *in vacuo* and the residue was washed with benzene (4 × 2 cm^3) and dried *in vacuo* at 80 °C to give compound **1** (96.2 mg, 94% yield) as a yellow powder, mp 220–222 °C (*cf.* lit.:[17] mp 215–216 °C); λ^{abs}_{max}(water)/nm ~356(sh), 318 and 275 (ε/M^{-1} cm^{-1} ~5800, 19 800 and 26 300); λ^{f}_{max}(water)/nm 472; δ_H (500.13 MHz; DMSO-d_6; 25 °C) 4.35 (3H, s, Me), 7.65–7.74 (2H, m, 6′-H, 7′-H), 8.06 (1H, br. d, ^3J 7.3, 5′-H), 8.12 (1H, br. d, ^3J 7.3, 8′-H),

8.16 (1H, dd, ^3J 8.5, ^4J 1.8, 3′-H), 8.18 (1H, d, ^3J 8.5, 4′-H), 8.65 (2H, d, ^3J 6.7, 3-H, 5-H), 8.77 (1H, br. s, 1′-H) and 9.05 (2H, d, ^3J 6.7, 2-H, 6-H); δ_C (125.76 MHz; DMSO-d_6; 25 °C) 46.97 (Me), 124.03 (3-C, 5-C, 3′-C), 127.21 (7′-C), 127.61 (5′-C), 128.42 (6′-C), 128.85 (1′-C), 129.02 (8′-C), 129.26 (4′-C), 130.58 (2′-C), 132.67 (8′a-C), 134.10 (4′a-C), 145.44 (2-C, 6-C) and 153.98 (4-C).

1-Methyl-4-(2-naphthyl)pyridinium perchlorate (**2**) was obtained according to a described procedure;[4c] δ_H (500.13 MHz; DMSO-d_6; 26 °C) 4.35 (3H, s, Me), 7.64–7.72 (2H, m, 6′-H, 7′-H), 8.05 (1H, d, ^3J 7.5, 5′-H), 8.11 (1H, d, ^3J 7.8, 8′-H), 8.15 (1H, dd, ^3J 8.7, ^4J 1.5, 3′-H), 8.18 (1H, d, ^3J 8.7, 4′-H), 8.63 (2H, d, ^3J 6.7, 3-H, 5-H), 8.76 (1H, br. s, 1′-H) and 9.04 (2H, d, ^3J 6.7, 2-H, 6-H); δ_C (125.76 MHz; DMSO-d_6; 26 °C) 46.96 (Me), 124.03 (3′-C), 124.08 (3-C, 5-C), 127.26 (7′-C), 127.65 (5′-C), 128.45 (6′-C), 128.86 (1′-C), 129.05 (8′-C), 129.31 (4′-C), 130.65 (2′-C), 132.71 (8′a-C), 134.13 (4′a-C), 145.48 (2-C, 6-C) and 154.07 (4-C).

1-Butyl-4-(2-naphthyl)pyridinium iodide (3). A solution of a mixture of 4-(2-naphthyl)pyridine (100 mg, 0.49 mmol) and 1-iodobutane (222 μdm^3, 1.95 mmol) in benzene (20 cm^3) was heated at 85 °C (oil bath) for 110 h. The reaction mixture was concentrated *in vacuo* (up to ∼ a half of volume), and hexane (10 cm^3) was added. The precipitate thus formed was filtered, washed with hexane (2 × 5 cm^3), and dried in air to give compound **3** (152 mg, 80% yield) as a yellowish powder, mp 158–160 °C (found: C, 58.79; H, 5.19; N, 3.69. Calc. for $C_{19}H_{20}IN$ (389.27): C, 58.62; H, 5.18; N, 3.60%); δ_H (500.13 MHz; DMSO-d_6; 26 °C) 0.95 (3H, t, ^3J 7.4, Me), 1.35 (2H, m, CH_2Me), 1.95 (2H, m, CH_2CH$_2$N), 4.60 (2H, t, ^3J 7.4, CH$_2$N), 7.65–7.73 (2H, m, 6′-H, 7′-H), 8.06 (1H, d, ^3J 7.9, 5′-H), 8.12 (1H, d, ^3J 7.9, 8′-H), 8.15–8.21 (2H, m, 3′-H, 4′-H), 8.68 (2H, d, ^3J 6.3, 3-H, 5-H), 8.79 (1H, s, 1′-H) and 9.15 (2H, d, ^3J 6.3, 2-H, 6-H); δ_C (125.76 MHz; DMSO-d_6; 25 °C) 13.25 (Me), 18.69 (*C*H$_2$Me), 32.49 (*C*H$_2$CH$_2$N), 59.54 (CH$_2$N), 124.08 (3′-C), 124.47 (3-C, 5-C), 127.21 (7′-C), 127.62 (5′-C), 128.45 (6′-C), 128.99 (1′-C), 129.04 (8′-C), 129.25 (4′-C), 130.61 (2′-C), 132.68 (8′a-C), 134.13 (4′a-C), 144.60 (2-C, 6-C) and 154.38 (4-C).

1-Butyl-4-(2-naphthyl)pyridinium perchlorate (4). Compound **3** (44 mg, 0.11 mmol) was dissolved with heating in abs. EtOH (2 cm^3), and conc. $HClO_4$ (70%, aq.) (20 μdm^3, 0.23 mmol) was added to the solution. The resulting solution was cooled down to −10 °C. The precipitate thus formed was filtered, washed with cold abs. EtOH (2 × 3 cm^3), and dried in air to give compound **4** (31 mg, 75% yield) as slightly yellowish thin-fibrous flakes, mp 150–152 °C (found: C, 62.27; H, 5.22; N, 3.96. Calc. for $C_{19}H_{20}ClNO_4 \cdot 0.25H_2O$ (366.32): C, 62.30; H, 5.64; N, 3.82%); δ_H (500.13 MHz; DMSO-d_6; 26 °C) 0.95 (3H, t, ^3J 7.4, Me), 1.35 (2H, m, CH_2Me), 1.95 (2H, m, CH_2CH$_2$N), 4.60 (2H, t, ^3J 7.4, CH$_2$N), 7.65–7.73 (2H, m, 6′-H, 7′-H), 8.06 (1H, d, ^3J 7.4, 5′-H), 8.12 (1H, d, ^3J 7.9, 8′-H), 8.15–8.21 (2H, m, 3′-H, 4′-H), 8.67 (2H, d, ^3J 6.0, 3-H, 5-H), 8.78 (1H, s, 1′-H) and 9.15 (2H, d, ^3J 6.0, 2-H, 6-H); δ_C (125.76 MHz; DMSO-d_6; 25 °C) 13.25 (Me), 18.73 (*C*H$_2$Me), 32.50 (*C*H$_2$CH$_2$N), 59.63 (CH$_2$N), 124.09 (3′-C), 124.50 (3-C, 5-C), 127.26 (7′-C), 127.65 (5′-C), 128.48 (6′-C), 128.99 (1′-C), 129.07 (8′-C), 129.30 (4′-C), 130.67 (2′-C), 132.71 (8′a-C), 134.16 (4′a-C), 144.62 (2-C, 6-C) and 154.47 (4-C).

3-[4-(2-Naphthyl)pyridinium-1-yl]propane-1-sulfonate (5). A solution of a mixture of 4-(2-naphthyl)pyridine (103 mg, 0.50 mmol) and 1,3-propanesultone (53 μdm^3, 0.60 mmol) in dry MeCN (3 cm^3) was kept at ambient temperature for 2 weeks. The precipitate thus formed was filtered and then extracted at 60 °C with dry acetone (7 cm^3) for 30 min. The insoluble substance was collected on a filter, washed with hot acetone (3 × 3 cm^3), and dried *in vacuo* at 80 °C to give betaine **5** (as a hydrate) (121 mg, 66% yield) as a yellowish powder, mp 273–274 °C (found: C, 58.77; H, 6.00; N, 3.87. Calc. for $C_{18}H_{17}NO_3S \cdot 2.25H_2O$ (367.93): C, 58.76; H, 5.89; N, 3.81%); δ_H (500.13 MHz; DMSO-d_6; 28 °C) 2.29 (2H, m, CH_2CH$_2$SO$_3$), 2.49 (2H, t, ^3J 7.1, CH$_2$SO$_3$), 4.75 (2H, t, ^3J 6.9, CH$_2$N), 7.65–7.72 (2H, m, 7′-H, 6′-H), 8.05 (1H, d, ^3J 7.5, 5′-H), 8.11 (1H, d, ^3J 8.0, 8′-H), 8.14–8.19 (2H, m, 3′-H, 4′-H), 8.65 (2H, d, ^3J 6.8, 3-H, 5-H), 8.77 (1H, s, 1′-H) and 9.15 (2H, d, ^3J 6.8, 2-H, 6-H); δ_C (125.76 MHz; DMSO-d_6; 26 °C) 27.21 (*C*H$_2$CH$_2$SO$_3$), 46.91 (CH$_2$SO$_3$), 58.66 (CH$_2$N), 124.13 (3′-C), 124.50 (3-C, 5-C), 127.22 (7′-C), 127.65 (5′-C), 128.43 (6′-C), 129.00 (1′-C), 129.07 (8′-C), 129.26 (4′-C), 130.79 (2′-C), 132.71 (8′a-C), 134.13 (4′a-C), 144.86 (2-C, 6-C) and 154.46 (4-C).

Complex (1)$_2$@CB[8]. A mixture of compound **1** (6.2 mg, 17.9 μmol) and CB[8]·14H$_2$O (14.1 mg, 8.9 μmol) in distilled water (7 cm^3) was heated under reflux with stirring up to complete dissolution of the components (∼1.5 h). The resulting solution was slowly evaporated at ambient temperature to a volume of ∼0.7 cm^3 (for a month). The yellowish crystals thus formed were decanted and dried *in vacuo* at 80 °C to give complex (**1**)$_2$@CB[8] (as a hydrate) (10.9 mg, 57% yield) as a yellowish powder, mp >380 °C (dec.) (found: C, 44.60; H, 3.99; N, 22.59. Calc. for $2C_{16}H_{14}IN \cdot C_{48}H_{48}N_{32}O_{16} \cdot 6.5H_2O$ (2140.59): C, 44.89; H, 4.19; N, 22.25%). The stoichiometry of the complex was confirmed by ^{1}H NMR spectroscopy data (see Fig. 7 and Fig. S11 in the ESI†).

Complex 2(5)·γ-CD. A solution of a mixture of compound **5** (hydrate) (5.0 mg, 13.6 μmol) and γ-CD·4.5H$_2$O (18.7 mg, 13.6 μmol) in distilled water (1 cm^3) was slowly evaporated at ambient temperature to a volume of ∼0.1 cm^3 (for a week). The druses of colorless thin-plate crystals thus formed were decanted and dried *in vacuo* at 80 °C to give the 2 : 1 complex of compound **5** with γ-CD (as a hydrate) (7.9 mg, 56% yield) as a yellowish powder, mp 242–245 °C (dec.) (found: C, 49.01; H, 6.14; N, 1.19. Calc. for $2C_{18}H_{17}NO_3S \cdot C_{48}H_{80}O_{40} \cdot 6H_2O$ (2060.01): C, 48.98; H, 6.17; N, 1.36%). The stoichiometry of the complex was confirmed by ^{1}H NMR spectroscopy data (see Fig. S12 in the ESI†).

Complex (5)$_2$@CB[8]. A mixture of compound **5** (hydrate) (8.3 mg, 22.6 μmol) and CB[8]·14H$_2$O (17.8 mg, 11.3 μmol) in distilled water (8 cm^3) was heated under reflux with stirring up to complete dissolution of the components (for ∼1.5 h). The resulting solution was slowly evaporated at ambient temperature to a volume of ∼6 cm^3 (for 5 days). The yellow crystals thus formed were decanted and dried *in vacuo* at 80 °C to give complex (**5**)$_2$@CB[8] (as a hydrate) (17.5 mg, 75% yield) as a yellow powder, mp >350 °C (dec.) (found: C, 48.39; H, 4.53; N, 23.17. Calc. for $2C_{18}H_{17}NO_3S \cdot C_{48}H_{48}N_{32}O_{16} \cdot 5H_2O$ (2073.97): C, 48.65;

H, 4.47; N, 22.96%). The stoichiometry of the complex was confirmed by ^{1}H NMR spectroscopy data (see Fig. S13 in the ESI†).

^{1}H NMR titration

The titration experiments were performed in a 10 : 1 (v/v) D_2O–MeCN-d_3 mixture at 25 °C. The stability constants of the inclusion complexes of compounds **2**, **4**, and **5** with cavitands were determined by analyzing the shifts of the proton signals of compounds **2**, **4**, and **5** ($\Delta\delta_H$) depending on the concentrations of the added cavitands. The total concentrations of compounds **2**, **4**, and **5** did not change being equal to $\sim 5 \times 10^{-4}$ M, and the cavitand concentrations were varied starting from zero (the maximum cavitand to naphthylpyridine derivative concentration ratio was ~6). The $\Delta\delta_H$ values were measured to an accuracy of 0.001 ppm, with allowance made for the correction for the shift of the signal of residual protons in MeCN-d_2. In the case of slow exchange on the ^{1}H NMR time scale, the average chemical shifts were calculated taking into account the integral intensities of corresponding signals. The stability constants of the complexes were calculated using the HYPNMR program[14] and are shown in Table 1.

Spectrophotometric and fluorescence titrations

The titration experiments were performed in deionized water (HPLC grade, Aldrich) at ambient temperature using 1 cm quartz cells. The fluorescence was excited at the wavelength, at which the free naphthylpyridine derivative and its inclusion complex with a cavitand have the same extinction. In the case of spectrophotometric titration, the total concentration of compounds **2**, **4**, and **5** was maintained constant at the 2×10^{-5} M level, whereas the concentration of cavitands was varied from 0 to 1.2×10^{-4} M (for CB[*n*]) and to 2.6×10^{-3} M (for CD). In the case of fluorescence titration, the total concentration of compounds **2**, **4**, and **5** was maintained constant being 1×10^{-6} M (for titration with CB[*n*]) and 1×10^{-5} M (for titration with CD), whereas the concentration of cavitands was varied from 0 to 9.1×10^{-6} M (for CB[*n*]) and to 2.8×10^{-3} M (for CD). The analysis of concentration dependences of absorption and fluorescence spectra and the calculations of stability constants of the complexes were carried out using the HypSpec program included in the Hyperquad software package.[16] The found spectral characteristics of compounds **2**, **4**, and **5** and their complexes with cavitands and the stability constants of these complexes are presented in Table 2.

X-ray crystallography

The crystals of structures **1**, **3**(1), and **5**·0.5C_6H_6·2H_2O were grown from MeCN solutions (in the presence of DMSO for betaine **5**), which were slowly saturated with benzene by the vapor diffusion method at ambient temperature. The crystals of other polymorphs, **3**(2) and **5**·4H_2O, were obtained by slow evaporation of aqueous solutions of mixtures of compound **3** and β-CD (or **3** and CB[8]) and compound **5** and β-CD. The crystals of two polymorphs of complex (**5**)$_2$@CB[8] were grown by slow evaporation of an aqueous solution of a 2 : 1 mixture of the components at ambient temperature.

The single crystals of all compounds were coated with perfluorinated oil and mounted on a Bruker SMART-CCD diffractometer [graphite monochromatized Mo-K_α radiation (λ = 0.71073 Å), ω scan mode] under a stream of cold nitrogen [T = 240(2) K for (**5**)$_2$@CB[8]·28.5H_2O (first polymorph) and T = 120(2) K for other structures]. The sets of experimental reflections were measured, and the structures were solved by direct methods and refined with anisotropic thermal parameters for all non-hydrogen atoms. In the case of iodides **1**·C_6H_6, **3**(1) and **3**(2), absorption corrections were applied using the SADABS method. The hydrogen atoms were fixed at calculated positions at carbon atoms and then refined with an isotropic approximation for **3**(1), **5**·0.5C_6H_6·2H_2O and **5**·4H_2O or by using a riding model for other structures. The hydrogen atoms of the water molecules of solvation in **5**·0.5C_6H_6·2H_2O and **5**·4H_2O were found from the Fourier syntheses and then refined isotropically. In other hydrated structures, water hydrogen atoms were not located.

Crystal data for **1**·C_6H_6: $C_{22}H_{20}IN$, M = 425.29, monoclinic, space group $P2_1/c$ (no. 14), yellow plate, a = 14.9470(8) Å, b = 19.1821(10) Å, c = 14.0976(8) Å, β = 113.239(1)°, V = 3714.1(3) Å^3, T = 120(2) K, Z = 8, μ = 1.726 mm^{-1}, ρ_{calc} = 1.521 g cm^{-3}, $2\theta_{max}$ = 58.00°, 40 387 reflections measured, 9859 unique (R_{int} = 0.0321), R_1 = 0.0334 (7285 reflections with $I > 2\sigma(I)$), wR_2 = 0.0698 (all data), goodness-on-fit on F^2 = 1.033, 637 parameters, min/max residual electron density = −0.928/1.114 ē Å^{-3}. One of the two independent organic cations is disordered over two positions with the occupancy ratio of 0.67 : 0.33. Two of the three independent benzene molecules of solvation are situated at the symmetry centers of the unit cell. Two benzene molecules are disordered over two positions with the occupancy ratios of 0.77 : 0.23 and 0.51 : 0.49. ISOR command was applied for the atoms of the disordered moieties in order to constrain their anisotropic thermal parameters.

Crystal data for **3**(1): $C_{19}H_{20}IN$, M = 389.26, monoclinic, space group $P2_1/c$ (no. 14), colourless plate, a = 15.8562(3) Å, b = 14.2979(3) Å, c = 15.3748(3) Å, β = 102.969(2)°, V = 3396.71(12) Å^3, T = 120(2) K, Z = 8, μ = 1.880 mm^{-1}, ρ_{calc} = 1.522 g cm^{-3}, $2\theta_{max}$ = 58.00°, 46 072 reflections measured, 8351 unique (R_{int} = 0.0463), R_1 = 0.0298 (6927 reflections with $I > 2\sigma(I)$), wR_2 = 0.0584 (all data), goodness-on-fit on F^2 = 1.040, 539 parameters, min/max residual electron density = −0.807/1.354 ē Å^{-3}. No constraints were applied.

Crystal data for **3**(2): $C_{19}H_{20}IN$, M = 389.26, monoclinic, space group $C2/c$ (no. 15), yellow block, a = 15.871(6) Å, b = 15.739(8) Å, c = 15.215(6) Å, β = 98.826(4)°, V = 3756(3) Å^3, T = 120(2) K, Z = 8, μ = 1.700 mm^{-1}, ρ_{calc} = 1.377 g cm^{-3}, $2\theta_{max}$ = 54.00°, 17 490 reflections measured, 4103 unique (R_{int} = 0.0760), R_1 = 0.1318 (1889 reflections with $I > 2\sigma(I)$), wR_2 = 0.4247 (all data), goodness-on-fit on F^2 = 1.085, 446 parameters, min/max residual electron density = −0.935/1.417 ē Å^{-3}. The conjugated moiety of organic cation is disordered over three positions with the occupancy ratio of 0.40 : 0.30 : 0.30. The *N*-butyl substituent is disordered over two positions with the occupancy ratio of 0.55 : 0.45. The iodide anion is disordered over five close positions with the occupancy ratio of 0.50 : 0.42 : 0.04 : 0.02 : 0.02.

AFIX 66, AFIX 116, SADI, and ISOR commands were applied to constrain the geometry of this strongly disordered structure and anisotropic thermal parameters of most atoms.

Crystal data for **5**·0.5C_6H_6·2H_2O: $C_{21}H_{24}NO_5S$, M = 402.47, triclinic, space group $P\bar{1}$ (no. 2), colourless block, a = 8.2091(3) Å, b = 9.6979(4) Å, c = 13.7643(5) Å, α = 72.984(1)°, β = 84.057(1)°, γ = 65.762(1)°, V = 955.28(6) Å^3, T = 120(2) K, Z = 2, μ = 0.203 mm^{-1}, ρ_{calc} = 1.399 g cm^{-3}, $2\theta_{max}$ = 57.99°, 8150 reflections measured, 4975 unique (R_{int} = 0.0587), R_1 = 0.0373 (4365 reflections with $I > 2\sigma(I)$), wR_2 = 0.1053 (all data), goodness-on-fit on F^2 = 1.069, 349 parameters, min/max residual electron density = −0.406/0.504 ē Å^{-3}. The benzene molecule of solvation is situated at the symmetry center of the unit cell. No constraints were applied.

Crystal data for **5**·4H_2O: $C_{18}H_{25}NO_7S$, M = 399.45, triclinic, space group $P\bar{1}$ (no. 2), yellow plate, a = 8.1522(8) Å, b = 9.6335(10) Å, c = 13.8091(14) Å, α = 73.187(2)°, β = 82.605(2)°, γ = 66.352(2)°, V = 950.86(17) Å^3, T = 120(2) K, Z = 2, μ = 0.211 mm^{-1}, ρ_{calc} = 1.395 g cm^{-3}, $2\theta_{max}$ = 57.99°, 10 493 reflections measured, 5016 unique (R_{int} = 0.0271), R_1 = 0.0465 (3622 reflections with $I > 2\sigma(I)$), wR_2 = 0.1225 (all data), goodness-on-fit on F^2 = 1.050, 344 parameters, min/max residual electron density = −0.316/0.602 ē Å^{-3}. No constraints were applied.

Crystal data for (**5**)$_2$@CB[8]·28.5H_2O: $C_{84}H_{139}N_{34}O_{50.5}S_2$, M = 2497.40, triclinic, space group $P\bar{1}$ (no. 2), yellow block, a = 14.460(15) Å, b = 15.020(15) Å, c = 15.044(15) Å, α = 67.677(16)°, β = 76.564(17)°, γ = 71.319(17)°, V = 2840(5) Å^3, T = 240(2) K, Z = 1, μ = 0.156 mm^{-1}, ρ_{calc} = 1.460 g cm^{-3}, $2\theta_{max}$ = 58.00°, 20 983 reflections measured, 14 240 unique (R_{int} = 0.0484), R_1 = 0.0832 (6237 reflections with $I > 2\sigma(I)$), wR_2 = 0.2613 (all data), goodness-on-fit on F^2 = 0.913, 846 parameters, min/max residual electron density = −0.385/0.900 ē Å^{-3}. This 2 : 1 complex is situated at the symmetry center. The naphthalene moiety of the guest molecule is disordered over two positions with the occupancy ratio of 0.51 : 0.49. AFIX 116 and ISOR commands were applied for the disordered fragment to constrain its geometry and anisotropic thermal parameters of its atoms. The numerous electron density peaks around the complex were assigned to oxygen atoms of water molecules of the solvation shell, and some of them are disordered or have incomplete occupancies.

Crystal data for (**5**)$_2$@CB[8]·15.7H_2O: $C_{84}H_{113.4}N_{34}O_{37.7}S_2$, M = 2266.80, tetragonal, space group $I4_1/a$ (no. 88), yellow block, a = b = 38.5719(14) Å, c = 14.8762(11) Å, V = 22133(2) Å^3, T = 120(2) K, Z = 8, μ = 0.144 mm^{-1}, ρ_{calc} = 1.361 g cm^{-3}, $2\theta_{max}$ = 58.00°, 119 809 reflections measured, 14 726 unique (R_{int} = 0.1218), R_1 = 0.1076 (7228 reflections with $I > 2\sigma(I)$), wR_2 = 0.3502 (all data), goodness-on-fit on F^2 = 1.107, 918 parameters, min/max residual electron density = −0.503/1.269 ē Å^{-3}. The 2 : 1 complex is situated at the symmetry center of the crystal unit cell. The guest molecule is disordered over two positions with the occupancy ratio of 0.52 : 0.48. AFIX 66, AFIX 116, SADI, and ISOR commands were applied for the disordered molecule. The numerous electron density peaks around the complex were assigned as oxygen atoms of water molecules of solvation, all of them having incomplete occupancies. ISOR command was applied for these atoms in order to constrain their anisotropic thermal parameters.

All the calculations were performed using the SHELXL software.[18] CCDC reference numbers 1867412 (**1**·C_6H_6), 1867413 (**3**(1)), 1867414 (**3**(2)), 1867415 (**5**·0.5C_6H_6·2H_2O), 1867416 (**5**·4H_2O), 1867417 ((**5**)$_2$@CB[8]·28.5H_2O), and 1867418 ((**5**)$_2$@CB[8]·15.7H_2O).†

Conflicts of interest

There are no conflicts to declare.

Acknowledgements

Financial support from the Russian Foundation for Basic Research (project 18-03-00214, in respect of NMR and electronic spectroscopy studies) and the Ministry of Science and Higher Education within the State assignment FSRC ''Crystallography and Photonics'' of RAS (in respect of synthesis of naphthylpyridine derivatives and their complexes) is gratefully acknowledged. L. G. K. thanks the Royal Society of Chemistry for an International Author grant (in respect of X-ray diffraction studies of naphthylpyridine derivatives). J. A. K. H. thanks the Engineering and Physical Sciences Research Council (EPSRC) for a Senior Research Fellowship (in respect of X-ray diffraction studies of complexes).

Notes and references

1 (*a*) J.-M. Lehn, *Supramolecular Chemistry. Concepts and Perspectives*, VCH, Weinheim, New York, Tokyo, 1995; (*b*) J. W. Steed and J. L. Atwood, *Supramol. Chem.*, Wiley, Chichester, New York, Weinheim, 2000; (*c*) *Modern Supramolecular Chemistry*, ed. F. Diederich, P. J. Stang and R. R. Tykwinski, Wiley-VCH, Weinheim, 2008; (*d*) H.-J. Schneider, *Angew. Chem., Int. Ed.*, 2009, **48**, 3924; (*e*) Yu. E. Alexeev, B. I. Kharisov, T. C. Hernández García and A. D. Garnovskii, *Coord. Chem. Rev.*, 2010, **254**, 794.

2 (*a*) K. Takahashi, *Chem. Rev.*, 1998, **98**, 2013; (*b*) D. M. Vriezema, M. Cormelass Aragonés, J. A. A. W. Elemans, J. J. L. M. Cornelissen, A. E. Rowan and R. J. M. Nolte, *Chem. Rev.*, 2005, **105**, 1445; (*c*) *Cyclodextrin Materials Photochemistry, Photophysics and Photobiology*, ed. A. Douhal, Elsevier, Amsterdam, London, New York, 2006; (*d*) G. V. Oshovsky, D. N. Reinhoudt and W. Verboom, *Angew. Chem., Int. Ed.*, 2007, **46**, 2366; (*e*) *Supramolecular Catalysis*, ed. P. W. N. M. Van Leeuwen, Wiley-VCH, Weinheim, 2008; (*f*) S. P. Gromov, *Russ. Chem. Bull.*, 2008, **57**, 1325; (*g*) *Molecular Encapsulation. Organic Reactions in Constrained Systems*, ed. U. H. Brinker and J.-L. Mieusset, Wiley, Chichester, 2010; (*h*) N. Vallavoju and J. Sivaguru, *Chem. Soc. Rev.*, 2014, **43**, 4084; (*i*) B. Bibal, C. Mongin and D. M. Bassani, *Chem. Soc. Rev.*, 2014, **43**, 4179; (*j*) S. Zarra, D. M. Wood, D. A. Roberts and J. R. Nitschke, *Chem. Soc. Rev.*, 2015, **44**, 419; (*k*) V. Ramamurthy and B. Mondal,

J. Photochem. Photobiol., C, 2015, **23**, 68; (*l*) S. Poplata, A. Tröster, Y.-Q. Zou and T. Bach, *Chem. Rev.*, 2016, **116**, 9748; (*m*) V. Ramamurthy and J. Sivaguru, *Chem. Rev.*, 2016, **116**, 9914.

3 (*a*) K. A. Connors, *Chem. Rev.*, 1997, **97**, 1325; (*b*) *Cyclodextrins and Their Complexes*, ed. H. Dodziuk, Wiley-VCH, Weinheim, 2006; (*c*) W. L. Mock, *Comprehensive Supramolecular Chemistry*, ed. J. L. Atwood, J. E. D. Davies, D. D. MacNicol and F. Vögtle, Pergamon, Oxford, 1996, vol. 2, pp. 477–493; (*d*) O. A. Gerasko, D. G. Samsonenko and V. P. Fedin, *Russ. Chem. Rev.*, 2002, **71**, 741; (*e*) J. W. Lee, S. Samal, N. Selvapalam, H.-J. Kim and K. Kim, *Acc. Chem. Res.*, 2003, **36**, 621; (*f*) J. Lagona, P. Mukhopadhyay, S. Chakrabarti and L. Isaacs, *Angew. Chem., Int. Ed.*, 2005, **44**, 4844; (*g*) L. Isaacs, *Chem. Commun.*, 2009, 619; (*h*) W. M. Nau, M. Florea and K. I. Assaf, *Isr. J. Chem.*, 2011, **51**, 559; (*i*) L. Isaacs, *Isr. J. Chem.*, 2011, **51**, 578; (*j*) E. Masson, X. Ling, R. Joseph, L. Kyeremeh-Mensah and X. Lu, *RSC Adv.*, 2012, **2**, 1213; (*k*) K. I. Assaf and W. M. Nau, *Chem. Soc. Rev.*, 2015, **44**, 394; (*l*) E. N. Ushakov and S. P. Gromov, *Russ. Chem. Rev.*, 2015, **84**, 787; (*m*) S. J. Barrow, S. Kasera, M. J. Rowland, J. del Barrio and O. A. Scherman, *Chem. Rev.*, 2015, **115**, 12320; (*n*) G. Wanjun, Z. Zhiyong and L. Simin, *Prog. Chem.*, 2016, **28**, 1732; (*o*) H. Bai, F. Lv, L. Liu and S. Wang, *Chem. – Eur. J.*, 2016, **22**, 11114.

4 (*a*) V. B. Nazarov, V. G. Avakyan, S. P. Gromov, M. V. Fomina, T. G. Vershinnikova and M. V. Alfimov, *Russ. Chem. Bull.*, 2004, **53**, 2525; (*b*) V. B. Nazarov, V. G. Avakyan, S. P. Gromov, A. I. Vedernikov, M. V. Fomina, T. G. Vershinnikova, V. Yu. Gak, N. A. Lobova, V. Yu. Rudyak and M. V. Alfimov, *Russ. Chem. Bull.*, 2010, **59**, 941; (*c*) S. P. Gromov, V. B. Nazarov, V. G. Avakyan, M. V. Fomina, A. I. Vedernikov, L. G. Kuz'mina, T. G. Vershinnikova, N. A. Lobova, V. Yu. Rudyak, M. V. Alfimov and J. A. K. Howard, *J. Photochem. Photobiol., A*, 2011, **217**, 87; (*d*) V. B. Nazarov, V. G. Avakyan, M. V. Fomina, A. I. Vedernikov, M. V. Alfimov and S. P. Gromov, *Russ. Chem. Bull.*, 2013, **62**, 2150.

5 (*a*) A. L. Koner and W. M. Nau, *Supramol. Chem.*, 2007, **19**, 55; (*b*) Y. Liu, C.-J. Li, D.-S. Guo, Z.-H. Pan and Z. Li, *Supramol. Chem.*, 2007, **19**, 517; (*c*) W. M. Nau, A. Hennig and A. L. Koner, *Springer Ser. Fluoresc.*, 2008, **4**, 185; (*d*) S. Gadde, E. K. Batchelor, J. P. Weiss, Y. Ling and A. E. Kaifer, *J. Am. Chem. Soc.*, 2008, **130**, 17114; (*e*) N. Kh. Petrov, D. A. Ivanov, D. V. Golubkov, S. P. Gromov and M. V. Alfimov, *Chem. Phys. Lett.*, 2009, **480**, 96; (*f*) R. N. Dsouza, U. Pischel and W. M. Nau, *Chem. Rev.*, 2011, **111**, 7941; (*g*) G. Parvari, O. Reany and E. Keinan, *Isr. J. Chem.*, 2011, **51**, 646; (*h*) L. S. Atabekyan, A. I. Vedernikov, V. G. Avakyan, N. A. Lobova, S. P. Gromov and A. K. Chibisov, *J. Photochem. Photobiol., A*, 2013, **253**, 52; (*i*) A. I. Vedernikov, N. A. Lobova, N. A. Aleksandrova and S. P. Gromov, *Russ. Chem. Bull.*, 2015, **64**, 2459; (*j*) M. V. Fomina, A. S. Nikiforov, V. G. Avakyan, A. I. Vedernikov, N. A. Kurchavov, L. G. Kuz'mina, Yu. A. Strelenko, J. A. K. Howard and S. P. Gromov, *J. Photochem. Photobiol., A*, 2018, **353**, 34.

6 (*a*) E. Arunkumar, C. C. Forbes and B. D. Smith, *Eur. J. Org. Chem.*, 2005, 4051; (*b*) A. C. Bhasikuttan, H. Pal and J. Mohanty, *Chem. Commun.*, 2011, **47**, 9959.

7 (*a*) S. Y. Jon, Y. H. Ko, S. H. Park, H.-J. Kim and K. Kim, *Chem. Commun.*, 2001, 1938; (*b*) M. Pattabiraman, A. Natarajan, L. S. Kaanumalle and V. Ramamurthy, *Org. Lett.*, 2005, **7**, 529; (*c*) M. V. S. N. Maddipatla, L. S. Kaanumalle, A. Natarajan, M. Pattabiraman and V. Ramamurthy, *Langmuir*, 2007, **23**, 7545; (*d*) R. Kaliappan, M. V. S. N. Maddipatla, L. S. Kaanumalle and V. Ramamurthy, *Photochem. Photobiol. Sci.*, 2007, **6**, 737; (*e*) N. Barooah, B. C. Pemberton and J. Sivaguru, *Org. Lett.*, 2008, **10**, 3339; (*f*) S. P. Gromov, A. I. Vedernikov, L. G. Kuz'mina, D. V. Kondratuk, S. K. Sazonov, Yu. A. Strelenko, M. V. Alfimov and J. A. K. Howard, *Eur. J. Org. Chem.*, 2010, 2587; (*g*) B. C. Pemberton, R. Raghunathan, S. Volla and J. Sivaguru, *Chem. – Eur. J.*, 2012, **18**, 12178; (*h*) M. V. S. N. Maddipatla, M. Pattabiraman, A. Natarajan, K. Srivastav, J. T. Mague and V. Ramamurthy, *Org. Biomol. Chem.*, 2012, **10**, 9219; (*i*) H. Asahara, T. Iwamoto, T. Kida and M. Akashi, *Tetrahedron Lett.*, 2013, **54**, 688; (*j*) H. Yang, Y. Liu, K. Liu, L. Yang, Z. Wang and X. Zhang, *Langmuir*, 2013, **29**, 12909; (*k*) D. A. Ivanov, N. Kh. Petrov, M. V. Alfimov, A. I. Vedernikov and S. P. Gromov, *High Energy Chem.*, 2014, **48**, 253.

8 (*a*) C. Yang, A. Nakamura, G. Fukuhara, Y. Origane, T. Mori, T. Wada and Y. Inoue, *J. Org. Chem.*, 2006, **71**, 3126; (*b*) L. Lei, L. Luo, X.-L. Wu, G.-H. Liao, L.-Z. Wu and C.-H. Tung, *Tetrahedron Lett.*, 2008, **49**, 1502; (*c*) X.-L. Wu, L. Luo, L. Lei, G.-H. Liao, L.-Z. Wu and C.-H. Tung, *J. Org. Chem.*, 2008, **73**, 491; (*d*) L. Luo, G.-H. Liao, X.-L. Wu, L. Lei, C.-H. Tung and L.-Z. Wu, *J. Org. Chem.*, 2009, **74**, 3506; (*e*) B. Chen, S.-F. Cheng, G.-H. Liao, X.-W. Li, L.-P. Zhang, C.-H. Tung and L.-Z. Wu, *Photochem. Photobiol. Sci.*, 2011, **10**, 1441.

9 N. Kh. Petrov, D. A. Ivanov, Yu. A. Shandarov, I. V. Kryukov, A. A. Ivanov, M. V. Alfimov, N. A. Lobova and S. P. Gromov, *Chem. Phys. Lett.*, 2016, **647**, 157.

10 L. G. Kuz'mina, A. I. Vedernikov, N. A. Lobova, J. A. K. Howard, Yu. A. Strelenko, V. P. Fedin, M. V. Alfimov and S. P. Gromov, *New J. Chem.*, 2006, **30**, 458.

11 N. Kh. Petrov, D. A. Ivanov, Yu. A. Shandarov, I. V. Kryukov, A. D. Svirida, V. G. Avakyan, M. V. Alfimov, N. A. Lobova and S. P. Gromov, *Chem. Phys. Lett.*, 2017, **673**, 99.

12 (*a*) H.-J. Schneider, F. Hacket, V. Rüdiger and H. Ikeda, *Chem. Rev.*, 1998, **98**, 1755; (*b*) K. Moon and A. E. Kaifer, *Org. Lett.*, 2004, **6**, 185; (*c*) V. J. Smith, D. Bogdan, M. R. Caira, M. Bogdan, S. A. Bourne and S. I. Fărcaş, *Supramol. Chem.*, 2010, **22**, 172; (*d*) M. A. Gamal-Eldin and D. H. Macartney, *Org. Biomol. Chem.*, 2013, **11**, 1234.

13 M. V. Rekharsky and Y. Inoue, *Chem. Rev.*, 1998, **98**, 1875.

14 C. Frassineti, S. Ghelli, P. Gans, A. Sabatini, M. S. Moruzzi and A. Vacca, *Anal. Biochem.*, 1995, **231**, 374.

15 (*a*) D. A. Ivanov, N. Kh. Petrov, E. A. Nikitina, M. V. Basilevsky, A. I. Vedernikov, S. P. Gromov and M. V. Alfimov, *J. Phys. Chem. A*, 2011, **115**, 4505; (*b*) Z. Li, S. Sun, F. Liu, Y. Pang, J. Fan, F. Song and X. Peng, *Dyes Pigm.*, 2012, **93**, 1401; (*c*) H. Zhang, L. Liu, C. Gao, R. Sun and Q. Wang, *Dyes Pigm.*, 2012, **94**, 266; (*d*) D. A. Ivanov, N. Kh. Petrov, A. A. Ivanov, M. V. Alfimov, A. I. Vedernikov and S. P. Gromov, *Chem. Phys. Lett.*, 2014, **610-611**, 91.
16 P. Gans, A. Sabatini and A. Vacca, *Talanta*, 1996, **43**, 1739.
17 S. P. Gromov and M. V. Fomina, *Russ. Chem. Bull.*, 2004, **53**, 901.
18 G. M. Sheldrick, *Acta Crystallogr., Sect. C: Struct. Chem.*, 2015, **71**, 3.